Tutorial 12:
Introduction to CNNs

Digital Image Processing (236860)

Agenda

- Intuition
- Neural networks
- Convolutional neural networks
- Deep learning for solving inverse problems

Reminder

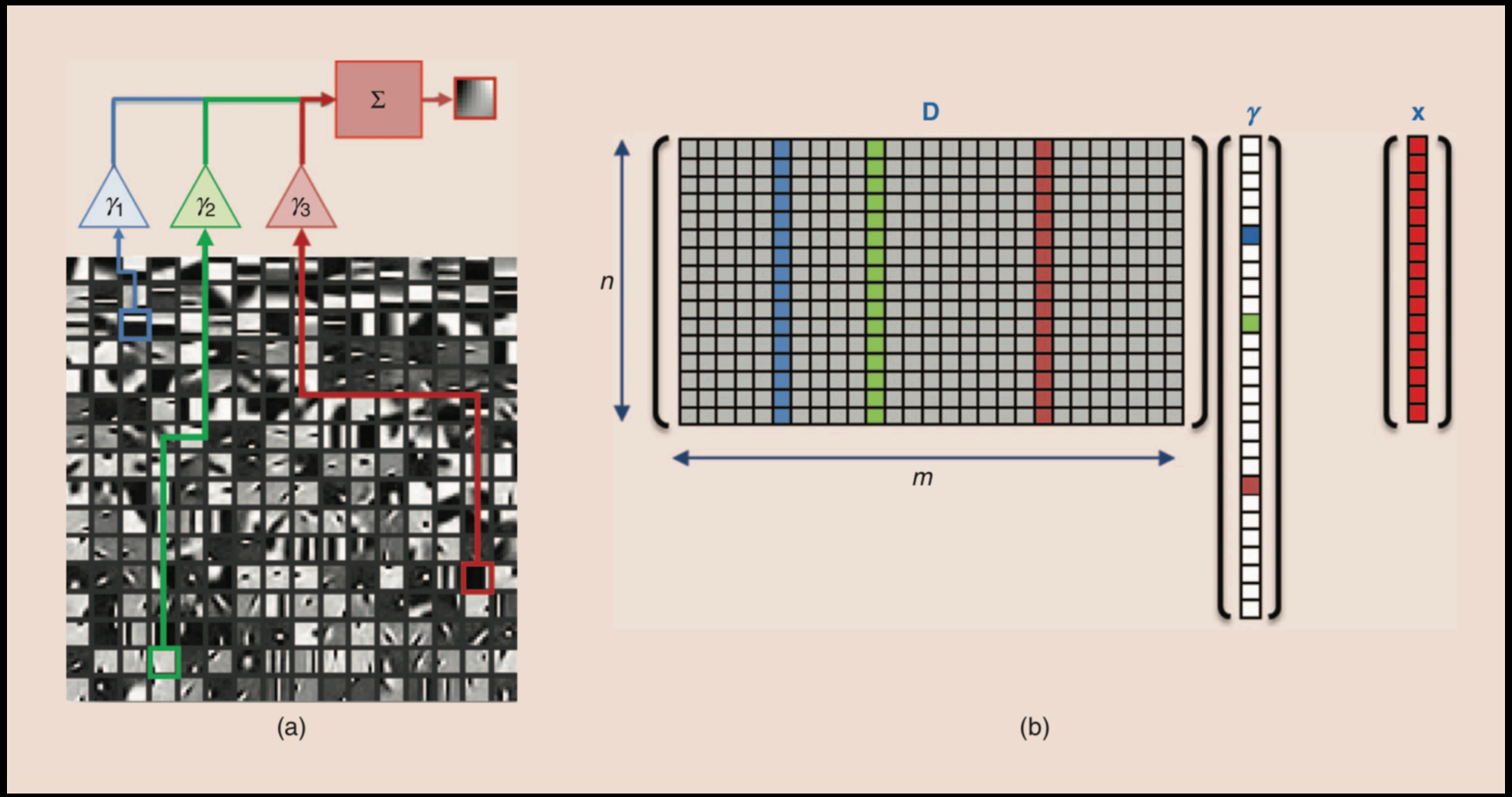

Papyan, Vardan, et al. "Theoretical Foundations of Deep Learning via Sparse Representations."

Difficulties of dictionary learning

- Slow (to train and to use)
- Cannot be used in high-dimensions (must work on patches)
- Why?
  - Too many degrees of freedom
  - Multiplying by $\boldsymbol{D}$ is costly
- Solution?
  - Force $\boldsymbol{D}$ to have a certain structure.

$$\mathbf{x} = \sum_{i=1}^{m} \mathbf{d}_i * \Gamma_i$$

Convolutional sparse coding (CSC)

$$\mathbf{X} = \sum_{i=1}^{m} \mathbf{C}_i \boldsymbol{\Gamma}_i = [\mathbf{C}_1 \ \mathbf{C}_2 \ \cdots \ \mathbf{C}_m] \begin{bmatrix} \boldsymbol{\Gamma}_1 \\ \boldsymbol{\Gamma}_2 \\ \vdots \\ \boldsymbol{\Gamma}_m \end{bmatrix} = \mathbf{D}\boldsymbol{\Gamma}.$$

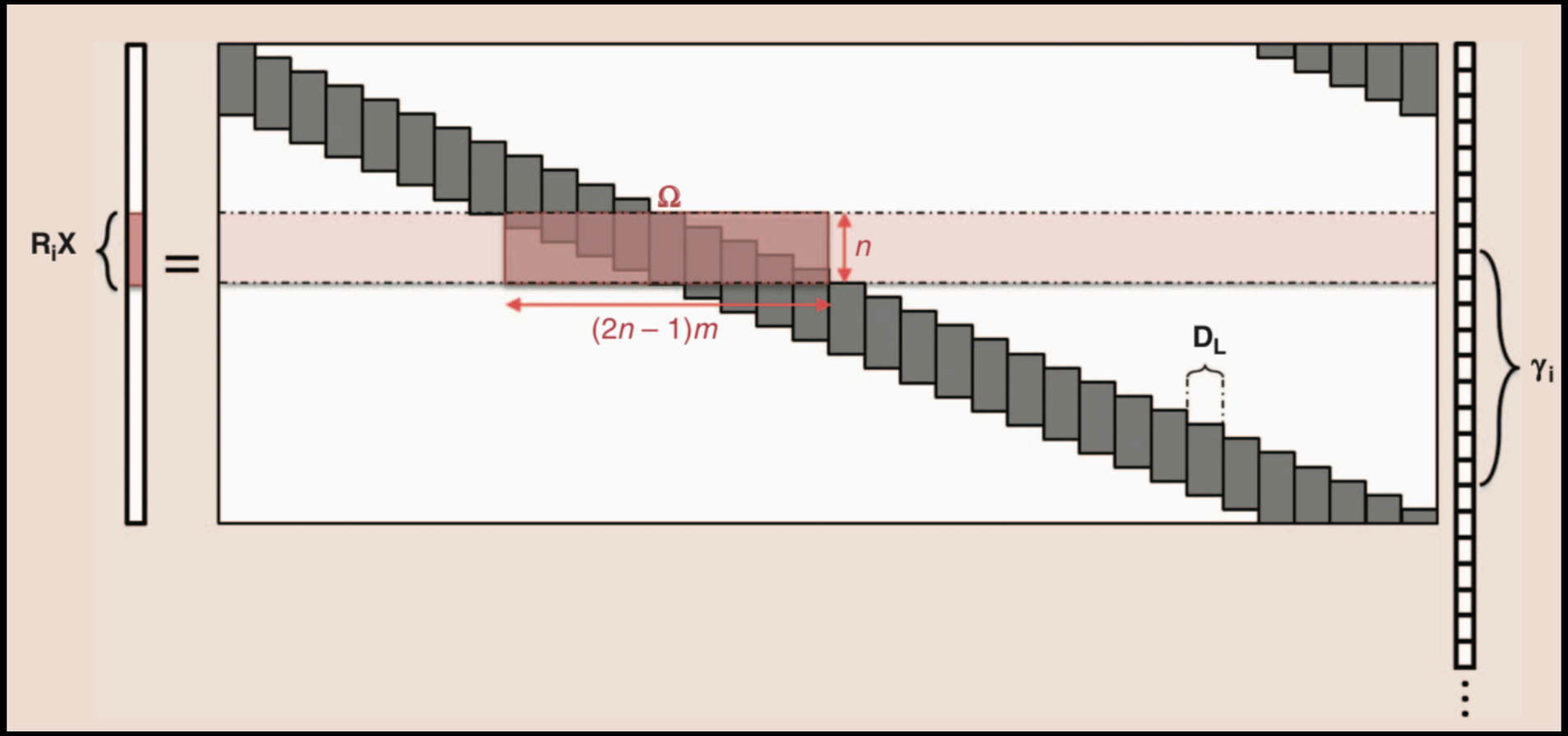

Papyan, Vardan, et al. "Theoretical Foundations of Deep Learning via Sparse Representations."

Multi-layered CSC (ML-CSC)

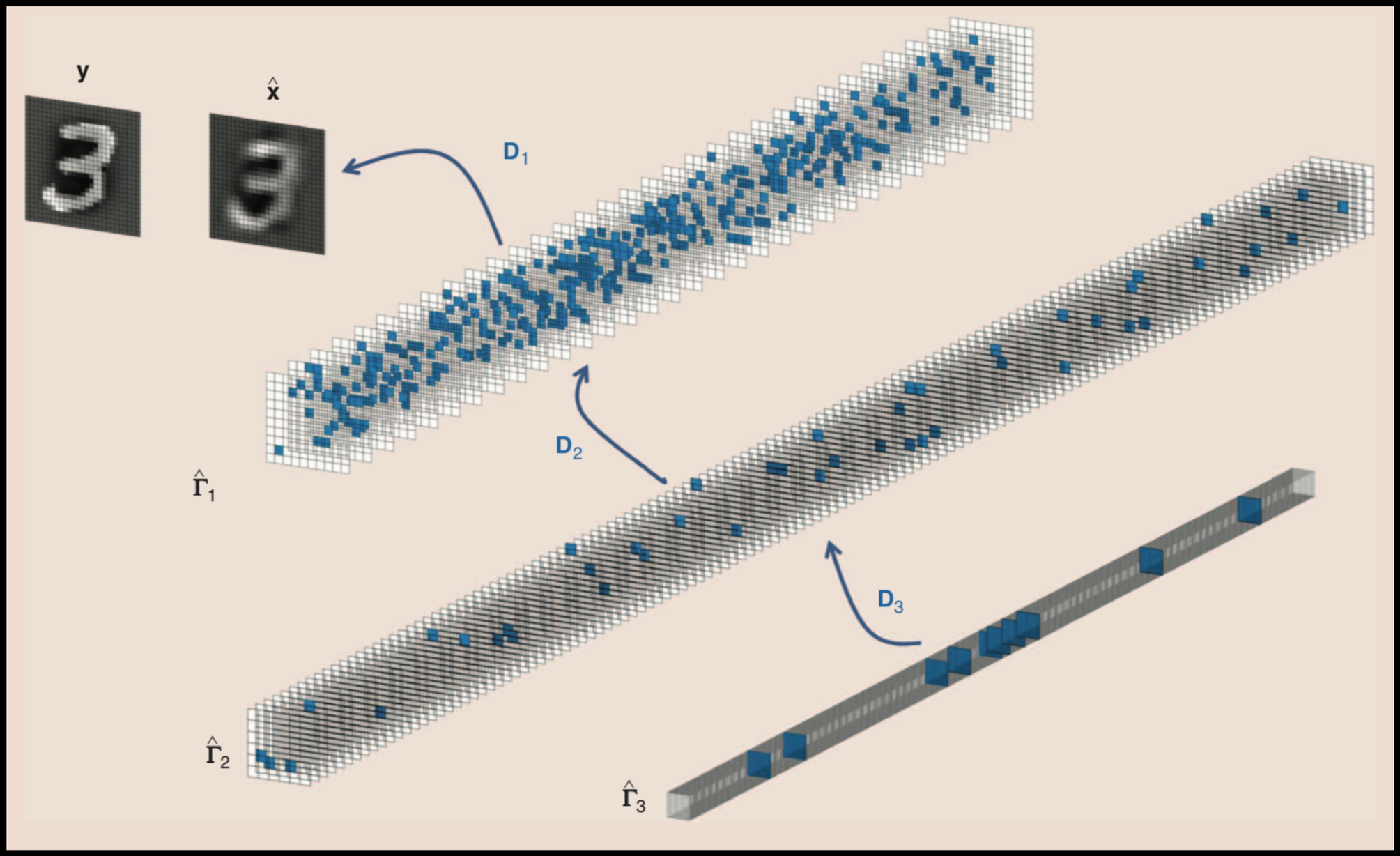

Papyan, Vardan, et al. "Theoretical Foundations of Deep Learning via Sparse Representations."

Multi-layered CSC (ML-CSC)

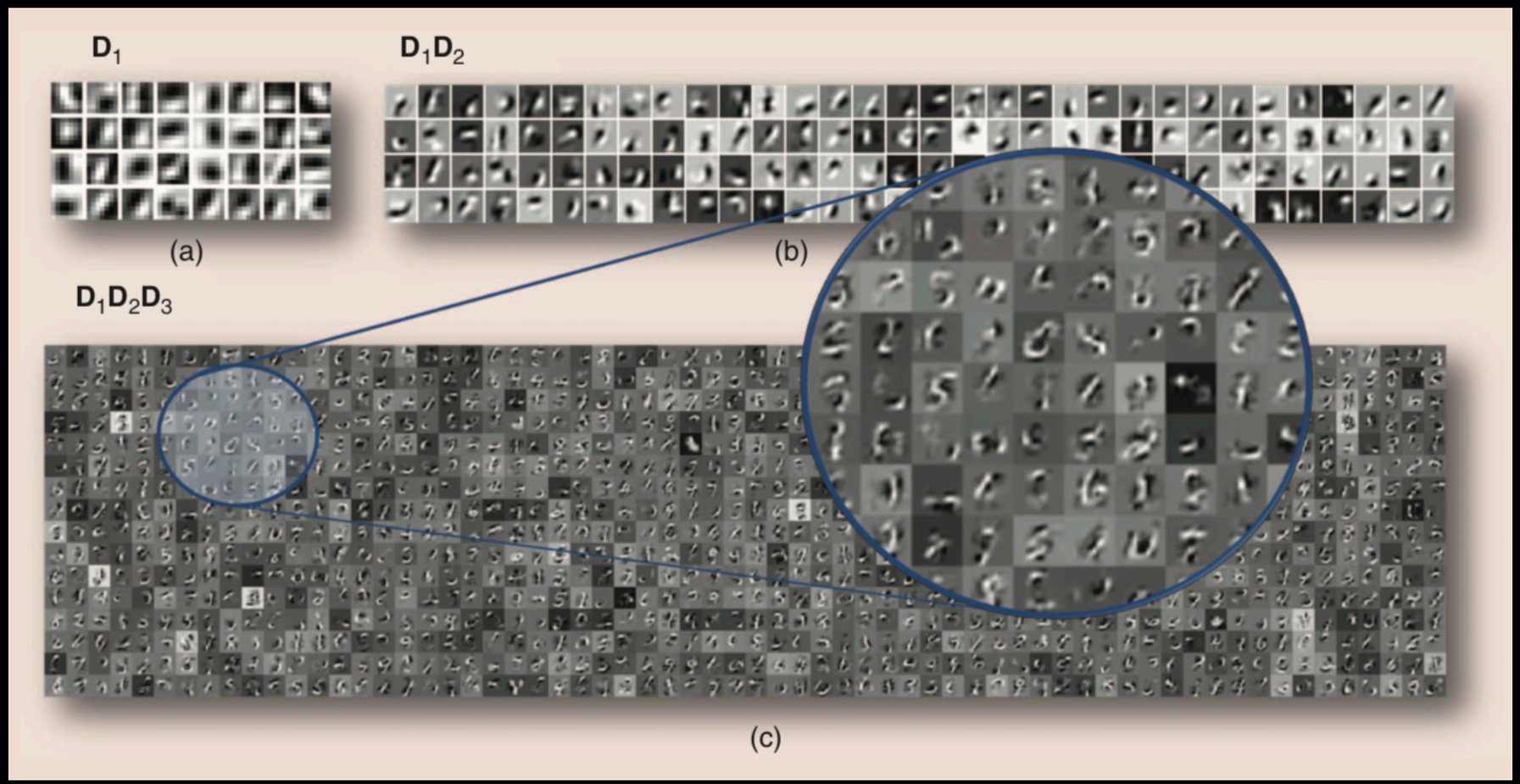

Papyan, Vardan, et al. "Theoretical Foundations of Deep Learning via Sparse Representations."

ISTA

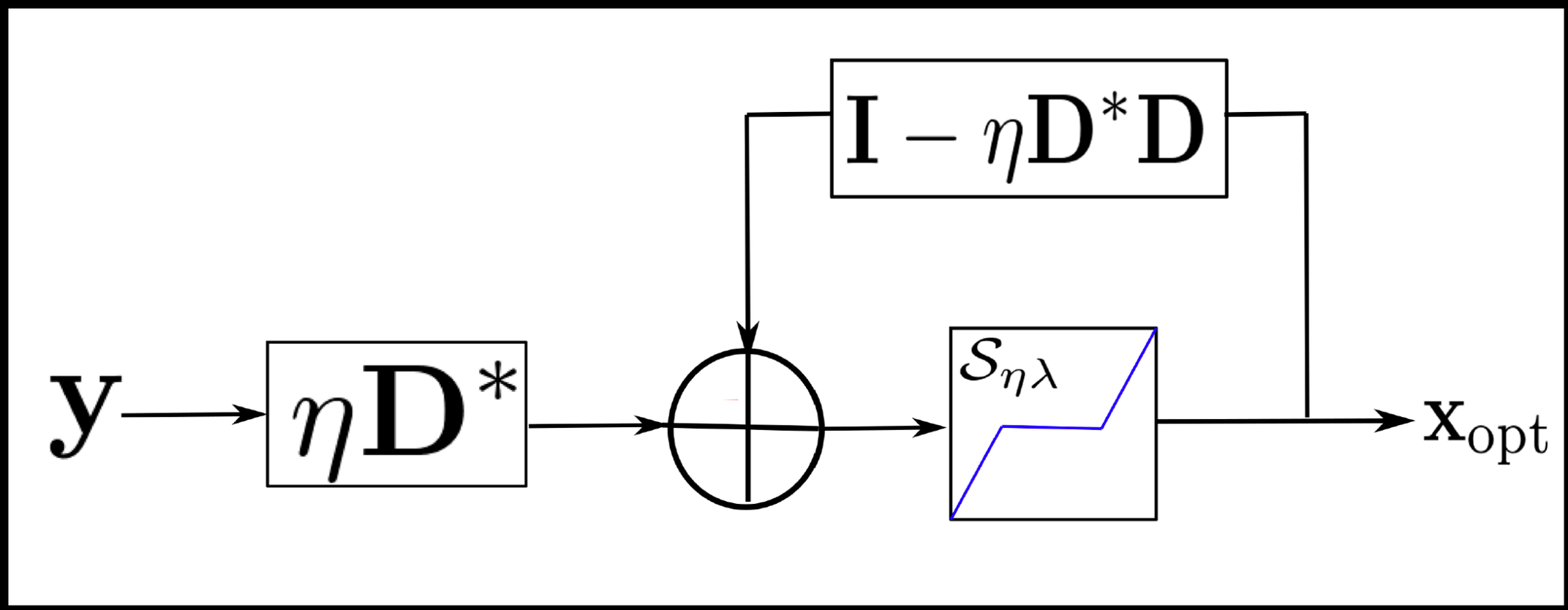
$\mathbf{I} - \eta \mathbf{D}^* \mathbf{D}$
$\mathbf{y}$
$\eta \mathbf{D}^*$
$\mathcal{S}_{\eta\lambda}$
$\mathbf{x}_{\text{opt}}$

Single iteration ISTA for CSC

VISTA Visual Sensing Theory & Applications Laboratory

Computer Science Department | Technion Israel Institute of Technology

First layer MAP estimator

$$\hat{\mathbf{c}}^1(y) = \arg\min_{\mathbf{c}^1 \geq 0} \frac{1}{2}\|y - \Phi^1\mathbf{c}^1\|_2^2 + \lambda_1\|\mathbf{c}^1\|_1 \qquad \Phi^1: \mathbf{c}^1 \to \sum_{k=1}^{K_1} \phi_k^1 * c_k^1$$

$$\hat{\mathbf{c}}^1(y) \approx \tilde{\mathbf{c}}^1(y) = \mathcal{S}^+_{\eta_1\lambda_1}(\eta_1\Phi^{1*}y) \qquad \Phi^{1*}: y \to \left(\bar{\phi}_1^1 * y, \dots, \bar{\phi}_{K_1}^1 * y\right)$$

$$= \mathcal{S}^+_{\lambda_1}(\Phi^{1*}y) = [\Phi^{1*}y - \lambda_1]_+$$

$$= \left([\bar{\phi}_1^1 * y - \lambda_1]_+, \dots, [\bar{\phi}_{K_1}^1 * y - \lambda_1]_+\right)$$

Single iteration ISTA for CSC

Next layer MAP estimator

$$\hat{\mathbf{c}}^k\left(\mathbf{c}^{k-1}\right) = \arg\min_{\mathbf{c}^k \geq \mathbf{0}} \frac{1}{2}\left\|\mathbf{c}^{k-1} - \mathbf{\Phi}^k \mathbf{c}^k\right\|_2^2 + \lambda_k \left\|\mathbf{c}^k\right\|_1$$

$$\hat{\mathbf{c}}^k\left(\mathbf{c}^{k-1}\right) \approx \tilde{\mathbf{c}}^k\left(\tilde{\mathbf{c}}^{k-1}\right) = \mathcal{S}^+_{\eta_k \lambda_k}\left(\eta_k \mathbf{\Phi}^{k*} \tilde{\mathbf{c}}^{k-1}\right)$$

$$= \left(\left[\bar{\boldsymbol{\phi}}_1^k * \tilde{\mathbf{c}}^{k-1} - \lambda_k\right]_+, \ldots, \left[\bar{\boldsymbol{\phi}}_{K_k}^k * \tilde{\mathbf{c}}^{k-1} - \lambda_k\right]_+\right)$$

$$= \left(\left[\sum_{i=1}^{K_{k-1}} \bar{\phi}_{1i}^k * \tilde{c}_i^{k-1} - \lambda_k\right]_+, \ldots, \left[\sum_{i=1}^{K_{k-1}} \bar{\phi}_{K_k i}^k * \tilde{c}_i^{k-1} - \lambda_k\right]_+\right)$$

Convolutional neural network (CNN)

Convolutional neural network (CNN)

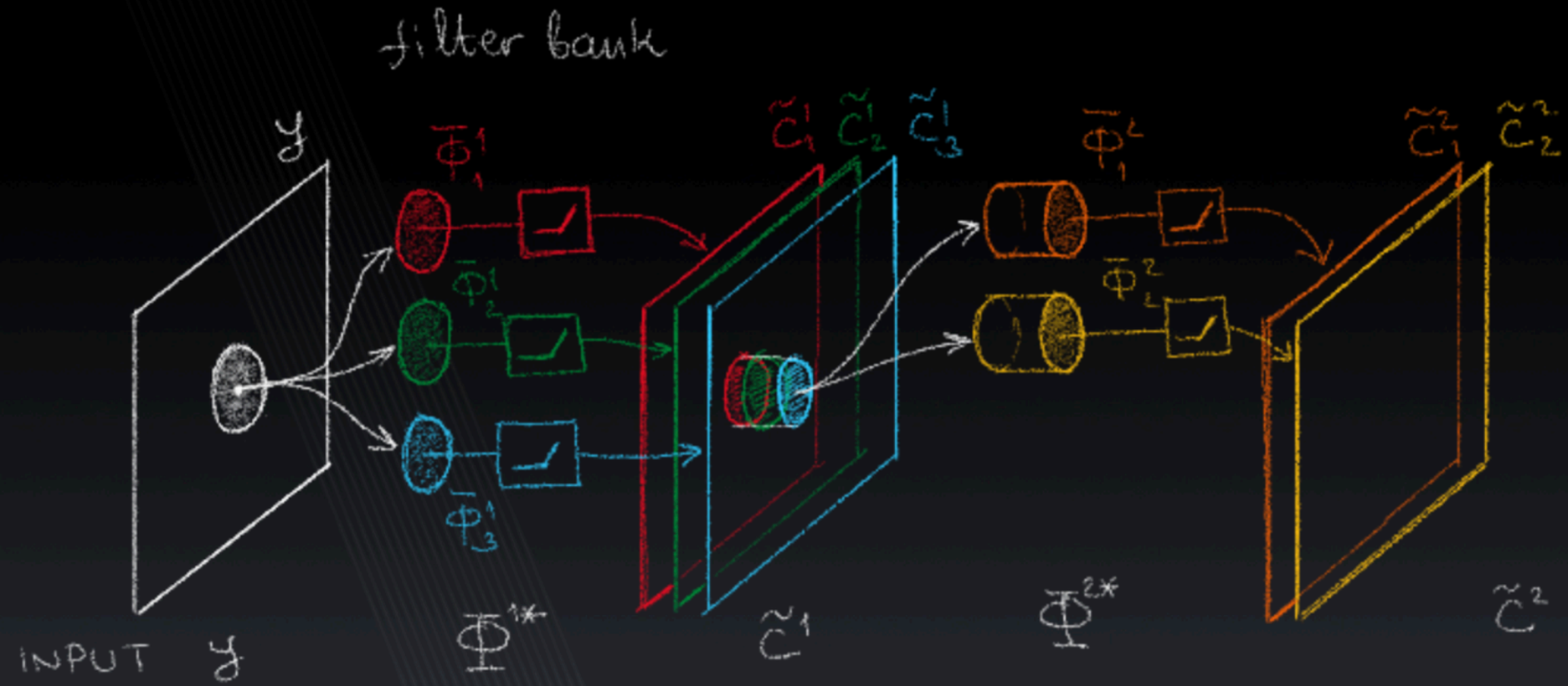

Encoder-decoder

Visual Sensing Theory & Applications Laboratory

Computer Science Department | Technion Israel Institute of Technology

Convolutional autoencoder

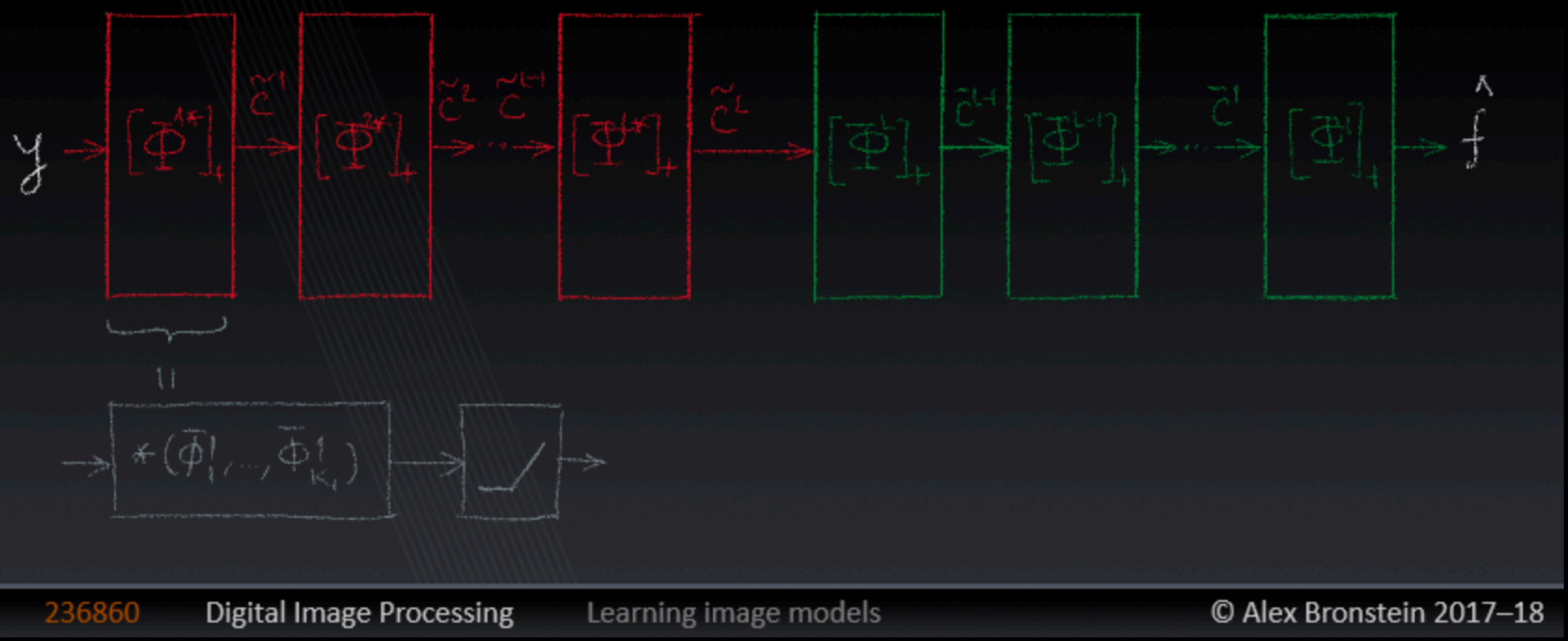

Back to our main interest

Inverse problems

Inverse problems

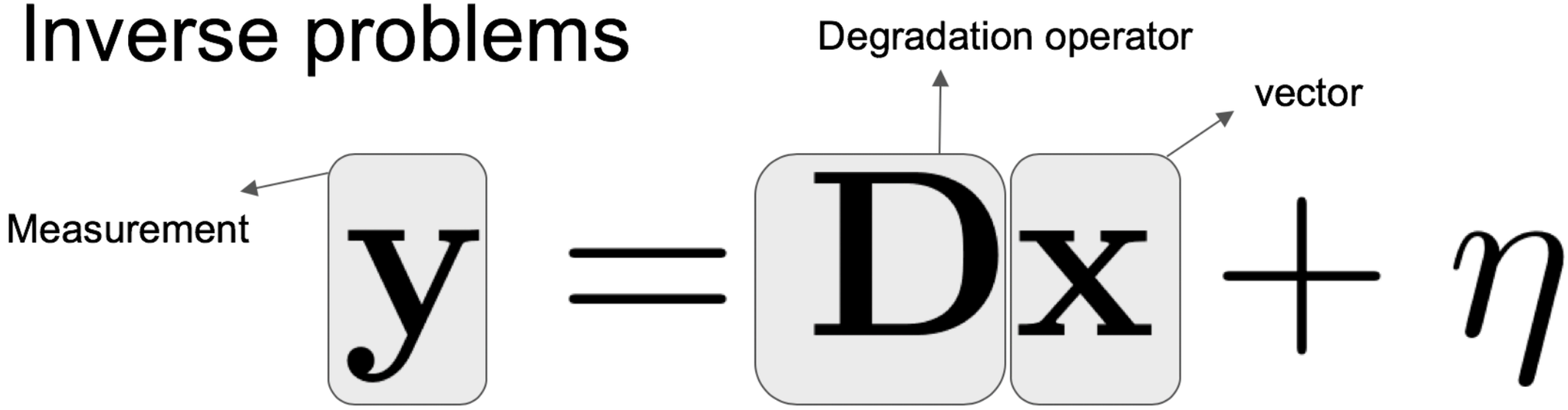

If D is:

1. Focal blur
2. Motion blur
3. Identity
4. Identity with missing values
5. Random gaussian matrix
6. Projection matrix

and so on…..

Then recovering x from y is:

1. Super-resolution
2. Deblurring
3. Denoising
4. Inpainting
5. Compressed sensing (x is sparse)
6. Tomography

and so on…..

Supervised learning

$$\mathbf{y} = \mathbf{D}\mathbf{x} + \eta$$

$\mathbf{y}$ – degraded image
$\mathbf{x}$ – clean image

Ideally, we would like to minimize the following risk:

$$\arg\min_{\theta} \mathbb{E}_{\mathbf{x}\sim p(\mathbf{x})}\, \ell(f_\theta(\mathbf{y}), \mathbf{x})$$

$f_\theta(.) =$ parametric inverse model $\quad \theta =$ parameters

Supervised learning

$$\mathbf{y} = \mathbf{D}\mathbf{x} + \eta$$

$\mathbf{y}$ – degraded image
$\mathbf{x}$ – clean image

Empirically, we do not have the distribution of **x,** but we do have access to a few examples. Then the loss function becomes:

$$\arg\min_{\theta} \sum_{i=1}^{N} \ell(f_\theta(\mathbf{y}_i), \mathbf{x}_i)$$

$f_\theta(.)$ = parametric inverse model $\quad \theta$ = parameters

Samples: $\{\mathbf{x}_i, \mathbf{y}_i\}_{i=1\ldots M}$

Neural networks

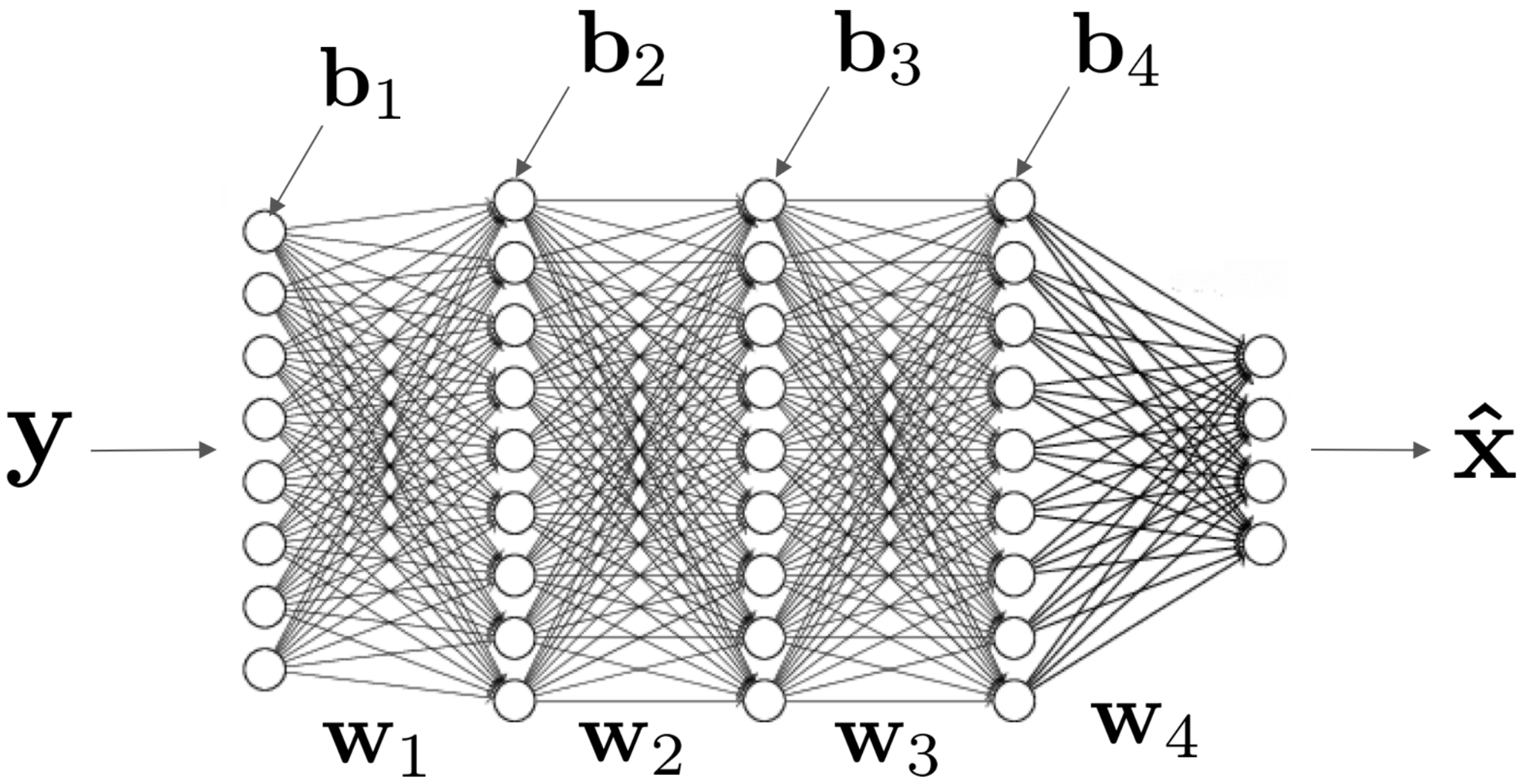

$$\hat{\mathbf{x}} = \mathbf{w}_4(\sigma(\mathbf{w}_3(\sigma(\mathbf{w}_2(\sigma(\mathbf{w}_1\mathbf{y} + \mathbf{b_1})) + \mathbf{b_2})) + \mathbf{b_3})) + \mathbf{b_4}$$

Activation functions

Sigmoid

$$\sigma(x) = \frac{1}{1+e^{-x}}$$

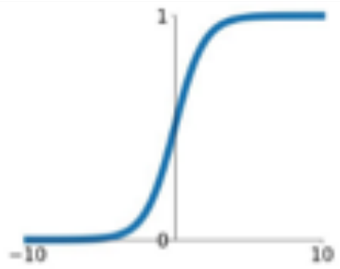

tanh

$$\tanh(x)$$

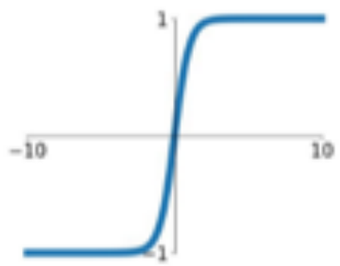

ReLU

$$\max(0, x)$$

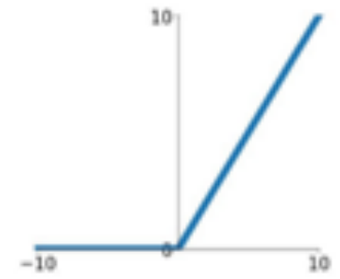

Leaky ReLU

$$\max(0.1x, x)$$

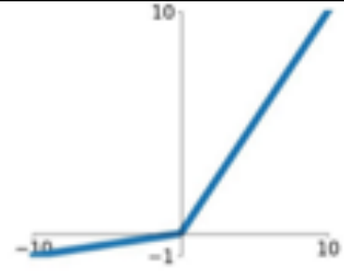

Maxout

$$\max(w_1^T x + b_1, w_2^T x + b_2)$$

ELU

$$\begin{cases} x & x \geq 0 \\ \alpha(e^x - 1) & x < 0 \end{cases}$$

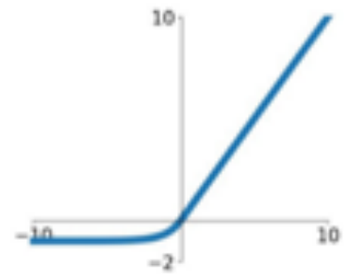

Image: © CS 231n, Stanford

Loss function

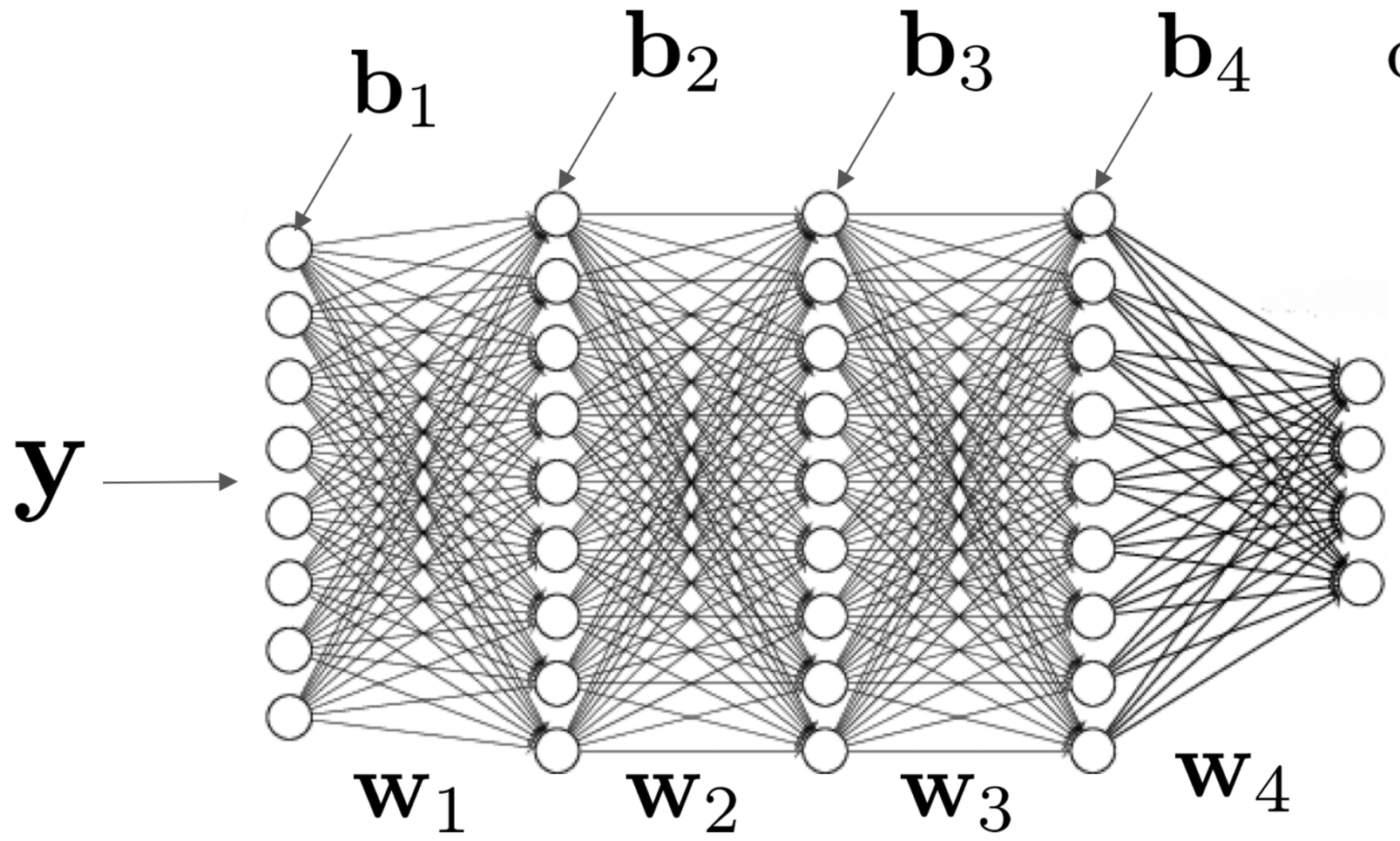

dataset: $\{\mathbf{x}_i, \mathbf{y}_i\}_{i=1\ldots M}$

$\theta = \{\mathbf{w}_{1..4}, \mathbf{b}_{1..4}\}$

$$\arg\min_{\theta} \sum_{i=1}^{N} \ell(\hat{\mathbf{x}}_i, \mathbf{x}_i)$$

$\ell(.)$ can be $\ell_1, \ell_2 \ldots$

$$\hat{\mathbf{x}} = \mathbf{w}_4(\sigma(\mathbf{w}_3(\sigma(\mathbf{w}_2(\sigma(\mathbf{w}_1\mathbf{y} + \mathbf{b_1})) + \mathbf{b_2})) + \mathbf{b_3})) + \mathbf{b_4}$$

Optimization

Gradient descent

Naïve optimization algorithm: gradient descent

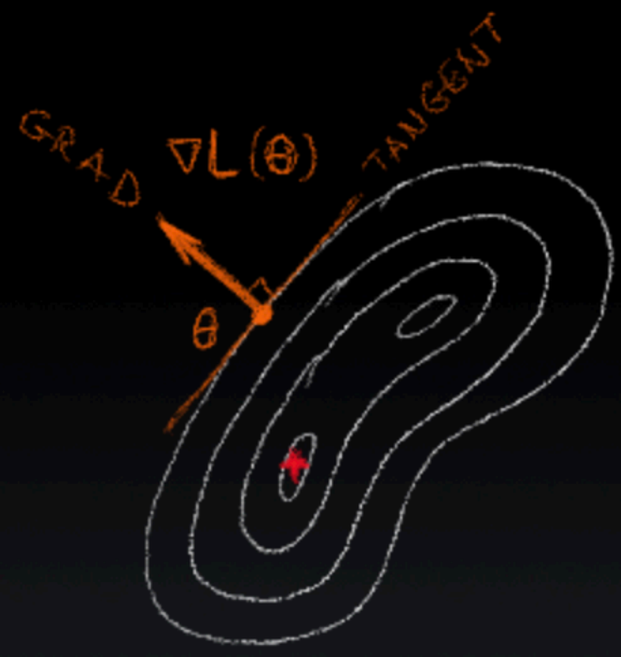

Initialization: start with some $\boldsymbol{\Theta}^0$

For $k = 1, \ldots$ **until convergence**

Update: $\boldsymbol{\Theta}^k \leftarrow \boldsymbol{\Theta}^{k-1} - \eta_k \nabla L(\boldsymbol{\Theta}^{k-1})$

Image denoising using fully-connected neural networks

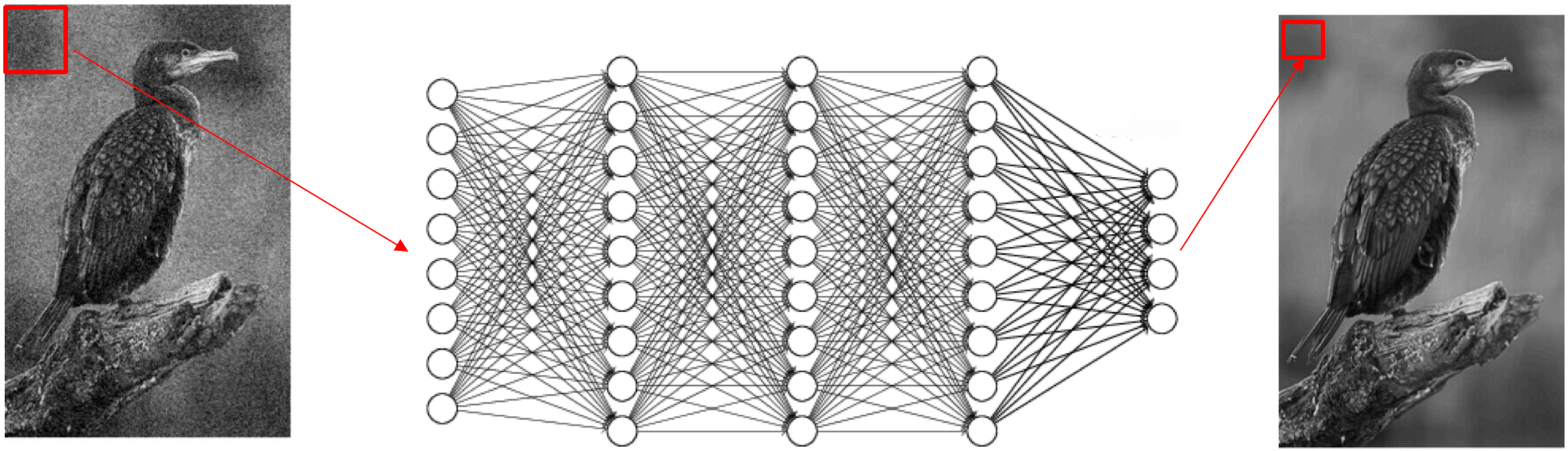

Burger et al., Image denoising: Can plain neural networks compete with BM3D?, CVPR 2012

Image denoising using fully-connected neural networks

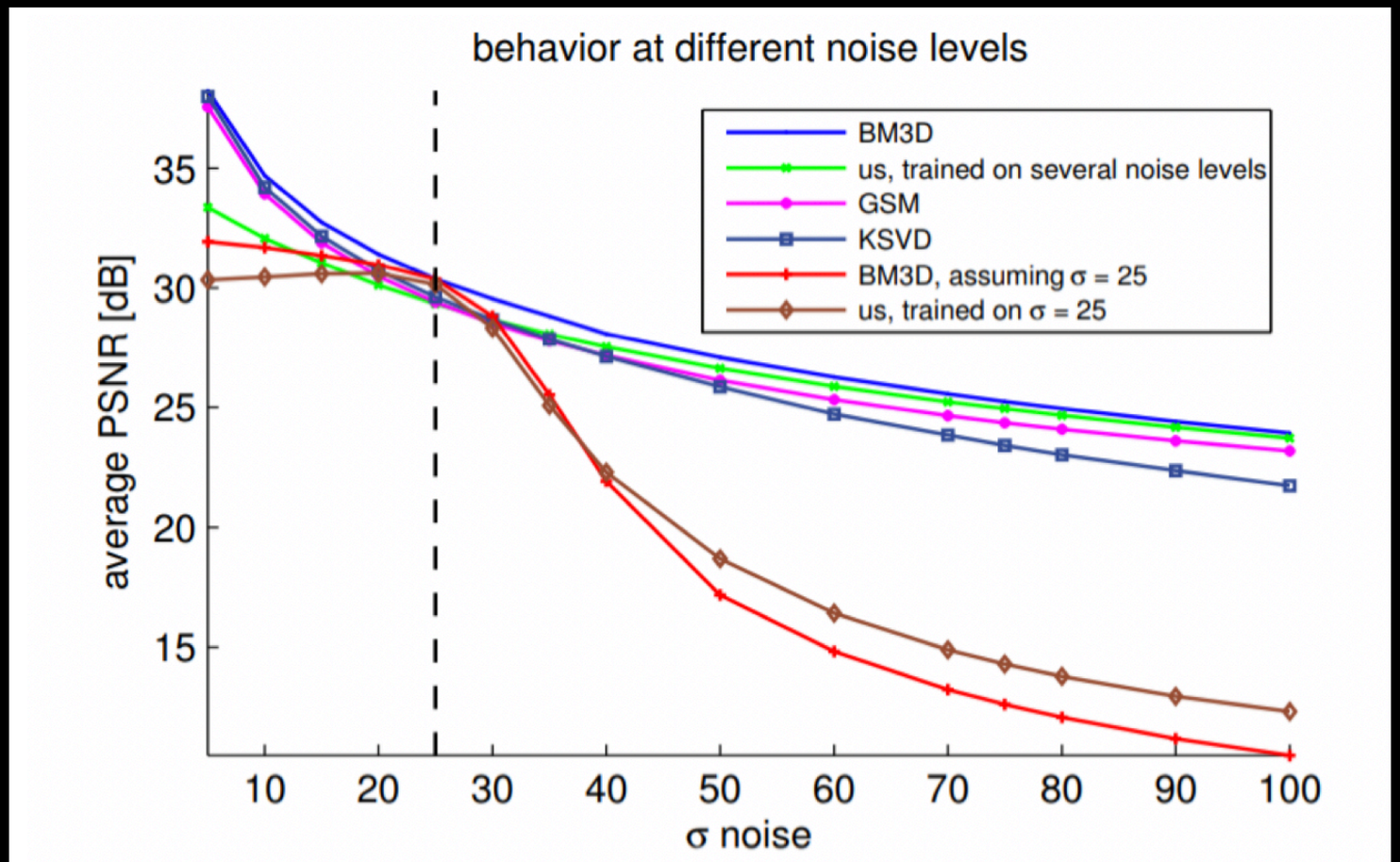

Figure 4. Comparison on images with various noise levels: the MLP trained for $\sigma = 25$ is competitive for $\sigma = 25$. The MLP trained on several noise levels is also competitive on higher noise levels.

Burger et al., Image denoising: Can plain neural networks compete with BM3D?, CVPR 2012

Problems

- Too many degrees of freedom.
- Slow and hard to train.
- High memory consumption.
- Each patch is being evaluated separately.
- The architecture doesn’t capture the spatial structure of an image.
- Solution?

Solution

Weight sharing

Different locations receive same processing

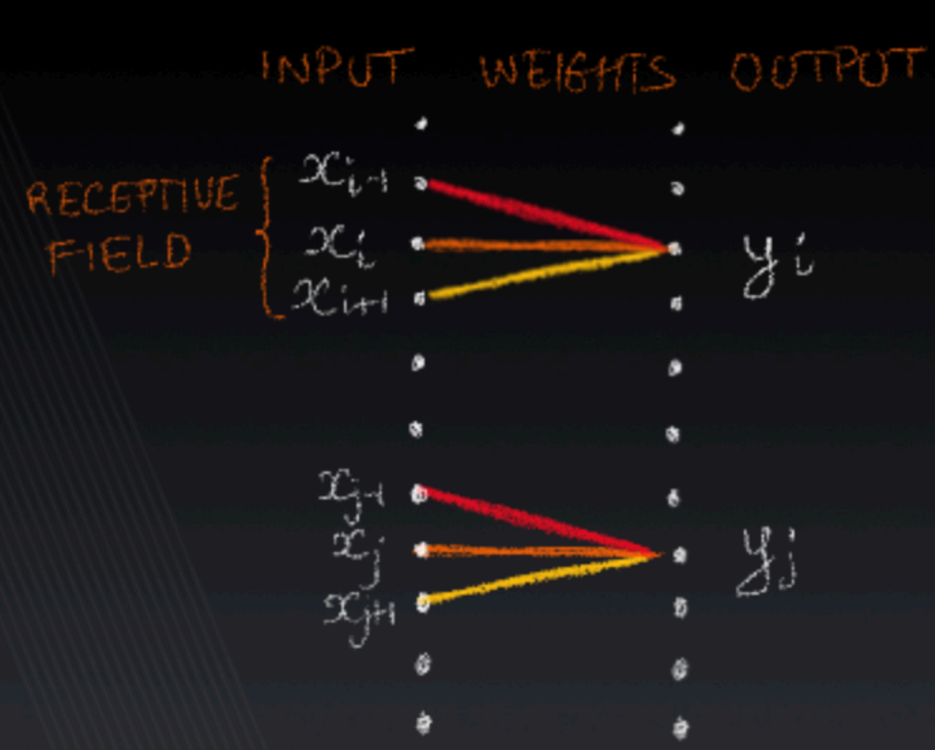

Convolutional neural networks (CNNs)

Convolutional layers

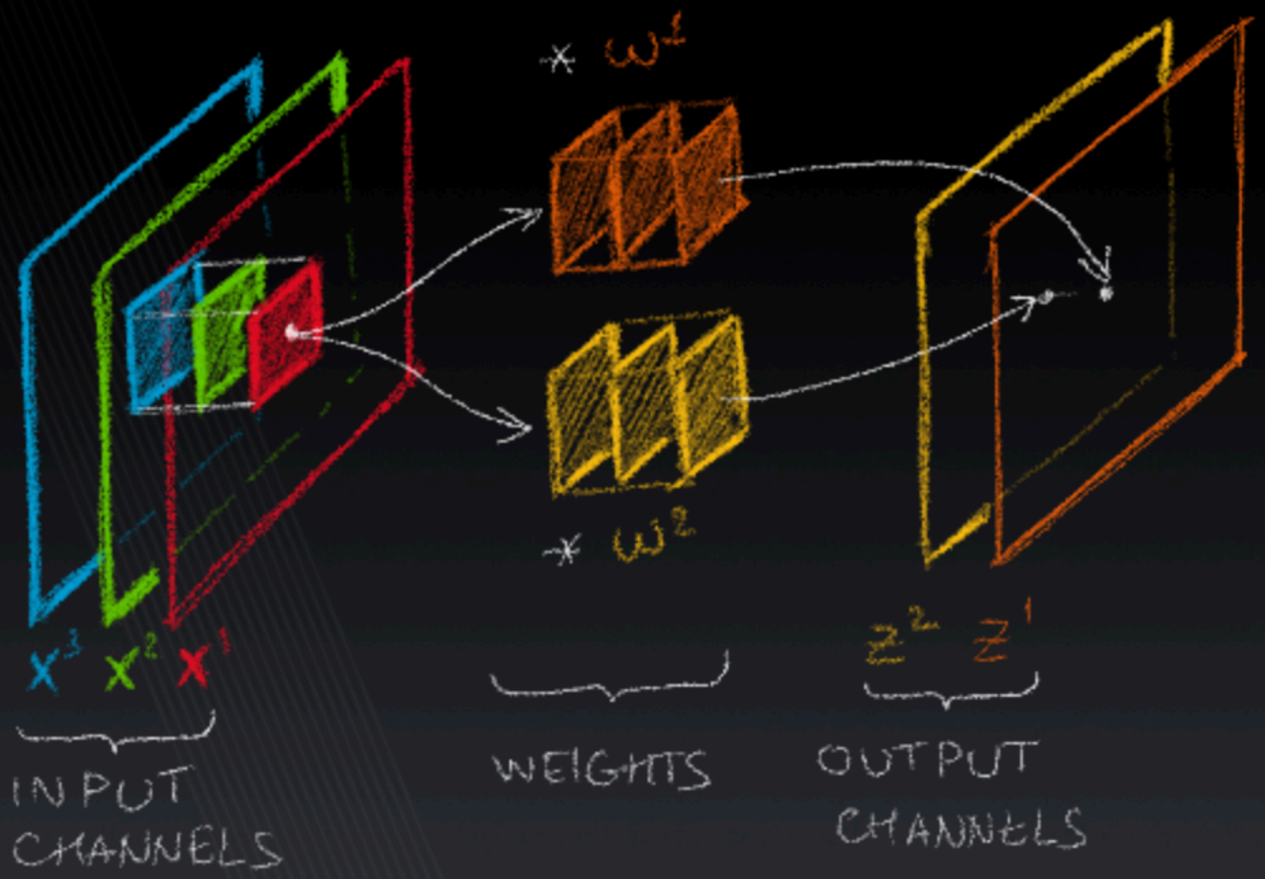

Pooling

Pooling

Break input into (possibly overlapping) **windows** $\{\mathbf{z}_{[i]}\}_{i=1}^{m}$

Apply a **transformation** to each window $\mathbf{y} = (\boldsymbol{\psi}(\mathbf{z}_{[1]}), \ldots, \boldsymbol{\psi}(\mathbf{z}_{[m]}))$

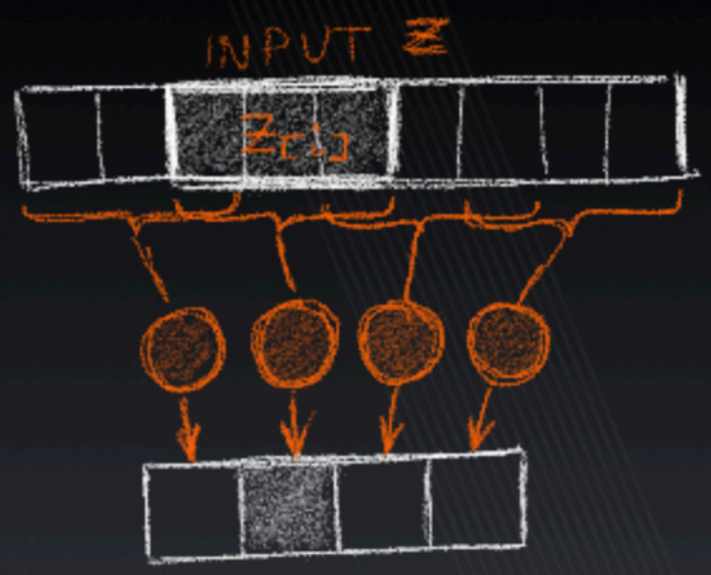

$\max \mathbf{z}_{[i]}$	**max pooling**
$\text{avg}\, \mathbf{z}_{[i]}$	**average pooling**
central sample of $\mathbf{z}_{[i]}$	**striding**

CNNs

- Repeating convolutions increase the receptive field.

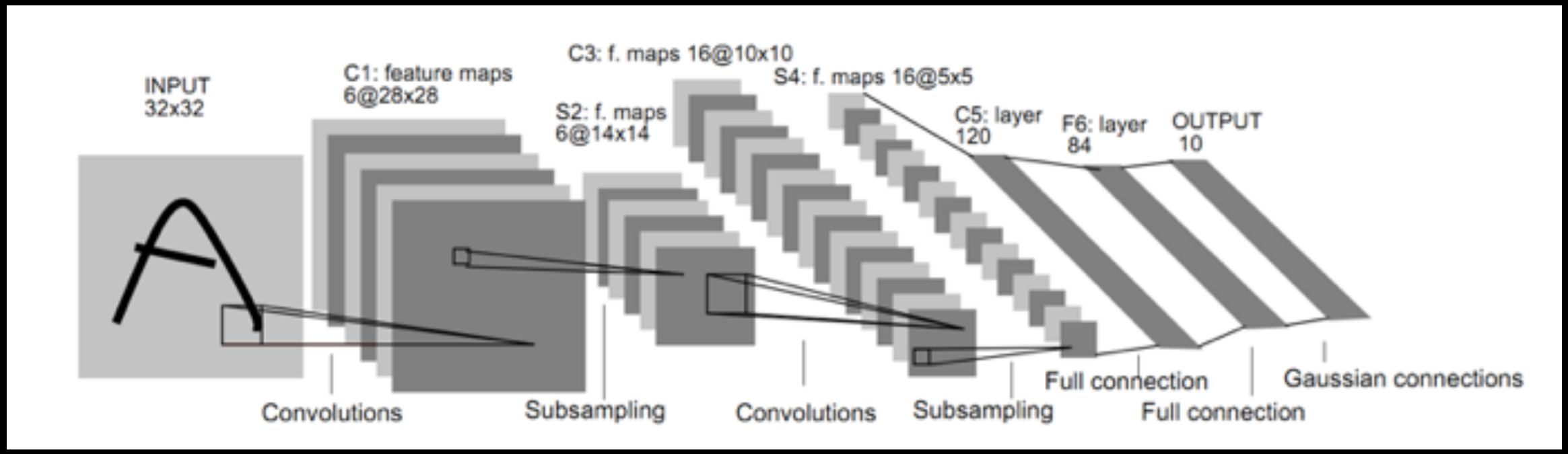

CNNs

- Convolutions capture local structure.
- Hierarchies of features can be obtained by stacking convolution layers.

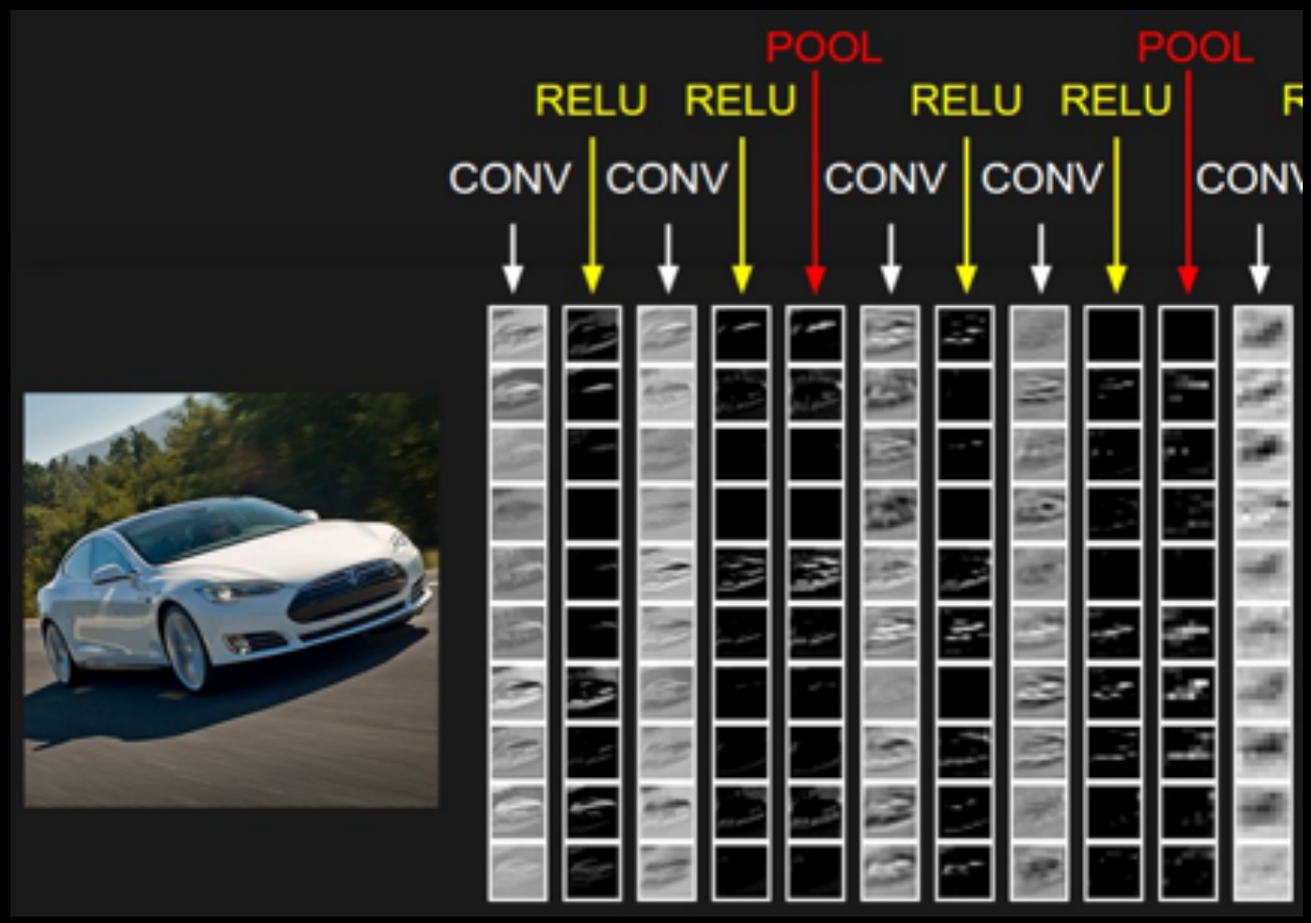

CNNs

- Each convolutions weight matrix is equivalent to a fully-connected network with the block diagonal structure.

- GPUs perform them efficiently as sparse matrix multiplication.

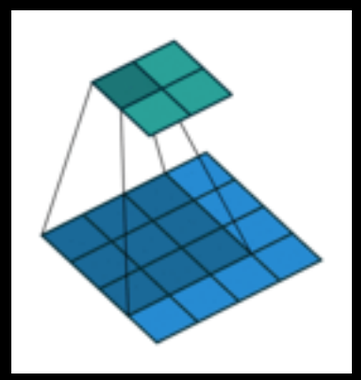

$$\begin{pmatrix} w_{0,0} & 0 & 0 & 0 \\ w_{0,1} & w_{0,0} & 0 & 0 \\ w_{0,2} & w_{0,1} & 0 & 0 \\ 0 & w_{0,2} & 0 & 0 \\ w_{1,0} & 0 & w_{0,0} & 0 \\ w_{1,1} & w_{1,0} & w_{0,1} & w_{0,0} \\ w_{1,2} & w_{1,1} & w_{0,2} & w_{0,1} \\ 0 & w_{1,2} & 0 & w_{0,2} \\ w_{2,0} & 0 & w_{1,0} & 0 \\ w_{2,1} & w_{2,0} & w_{1,1} & w_{1,0} \\ w_{2,2} & w_{2,1} & w_{1,2} & w_{1,1} \\ 0 & w_{2,2} & 0 & w_{1,2} \\ 0 & 0 & w_{2,0} & 0 \\ 0 & 0 & w_{2,1} & w_{2,0} \\ 0 & 0 & w_{2,2} & w_{2,1} \\ 0 & 0 & 0 & w_{2,2} \end{pmatrix}^T$$

Encoder-decoder

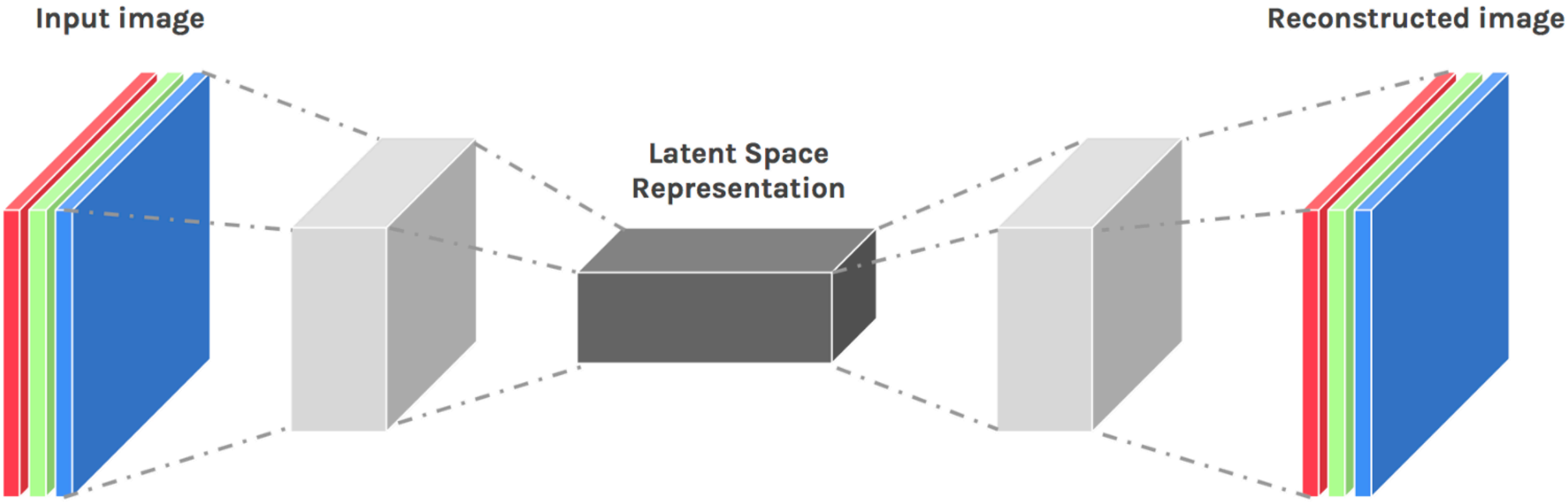

https://hackernoon.com/autoencoders-deep-learning-bits-1-11731e200694

Encoder-decoder with skip connections

- $Y = X + \eta$
- Instead of learning to approximate X, learn to approximate the noise $Y - X$.

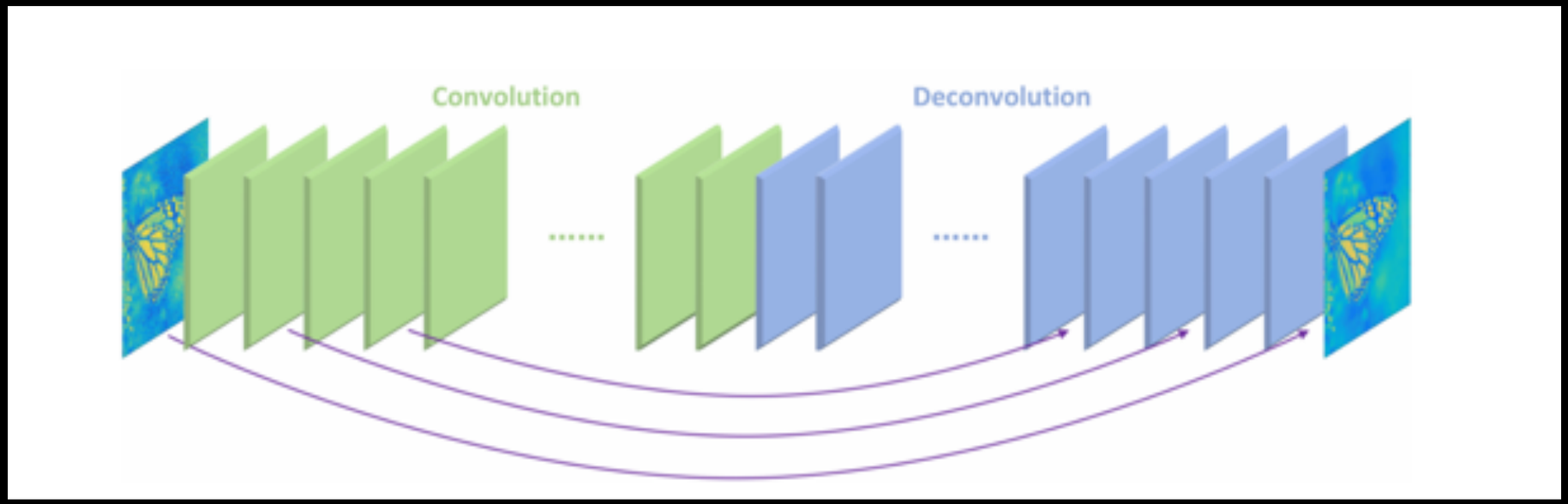

Mao et al., NIPS 2016

Image denonising

Table 1: Average PSNR and SSIM results of σ 10, 30, 50, 70 for the 14 images.

	PSNR								
	BM3D	EPLL	NCSR	PCLR	PGPD	WNNM	RED10	RED20	RED30
$\sigma = 10$	34.18	33.98	34.27	34.48	34.22	34.49	34.62	34.74	**34.81**
$\sigma = 30$	28.49	28.35	28.44	28.68	28.55	28.74	28.95	29.10	**29.17**
$\sigma = 50$	26.08	25.97	25.93	26.29	26.19	26.32	26.51	26.72	**26.81**
$\sigma = 70$	24.65	24.47	24.36	24.79	24.71	24.80	24.97	25.23	**25.31**
	SSIM								
$\sigma = 10$	0.9339	0.9332	0.9342	0.9366	0.9309	0.9363	0.9374	0.9392	**0.9402**
$\sigma = 30$	0.8204	0.8200	0.8203	0.8263	0.8199	0.8273	0.8327	0.8396	**0.8423**
$\sigma = 50$	0.7427	0.7354	0.7415	0.7538	0.7442	0.7517	0.7571	0.7689	**0.7733**
$\sigma = 70$	0.6882	0.6712	0.6871	0.6997	0.6913	0.6975	0.7012	0.7177	**0.7206**

Mao et al., NIPS 2016

Low-dose CT reconstruction

- Convert “low-dose” CT image to a “high-dose” one.

- Less dose = less energy of X-rays entering the body = less ionising radiation.

- Dataset synthetically generated using Poisson noise.

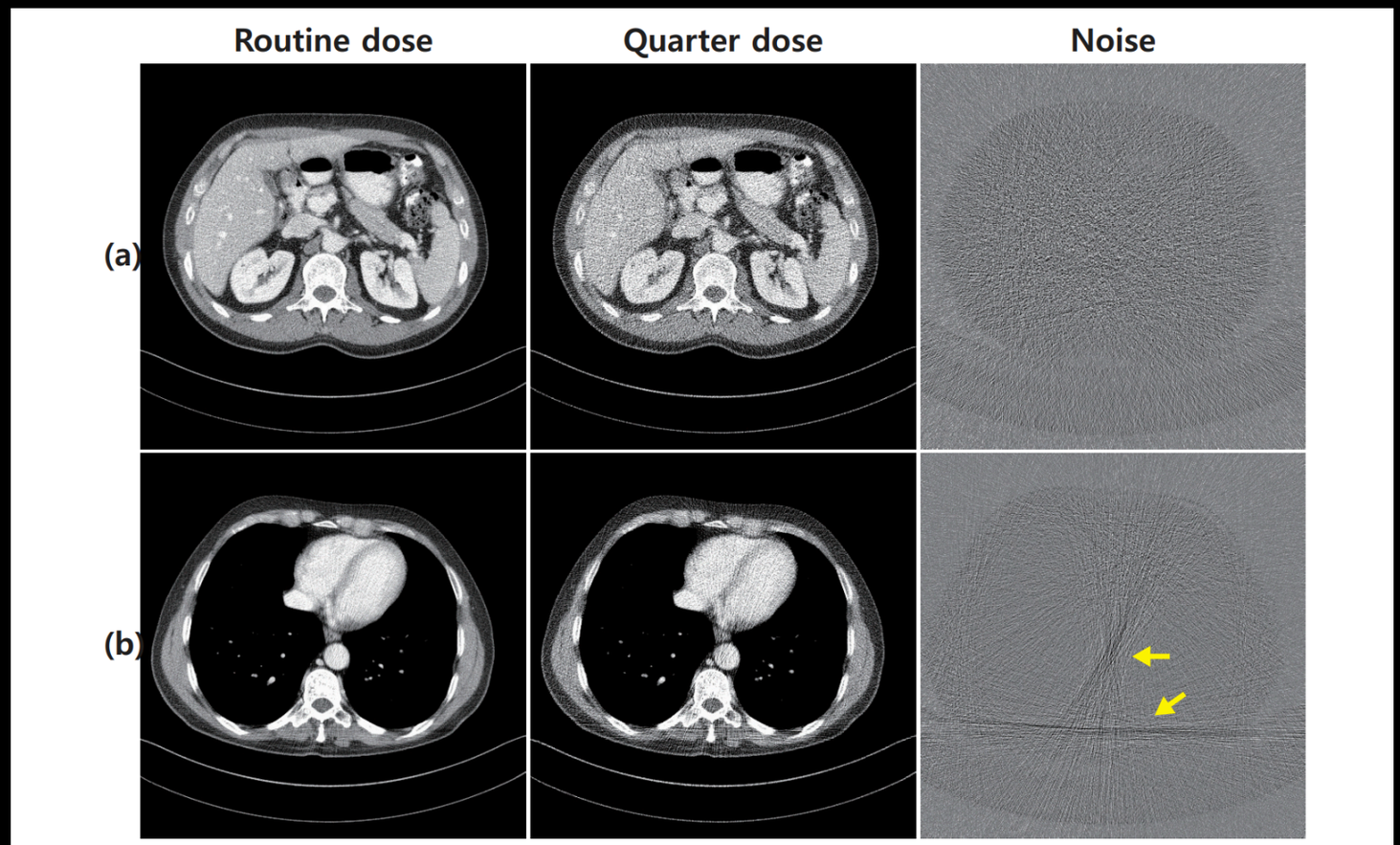

FIG. 1 Various noise patterns in low-dose CT images: (a) Gaussian noise, and (b) streaking artifacts

Kang et al., A deep CNN for Low-dose CT reconstruction, Medical Physics, 2017

Low-dose CT reconstruction

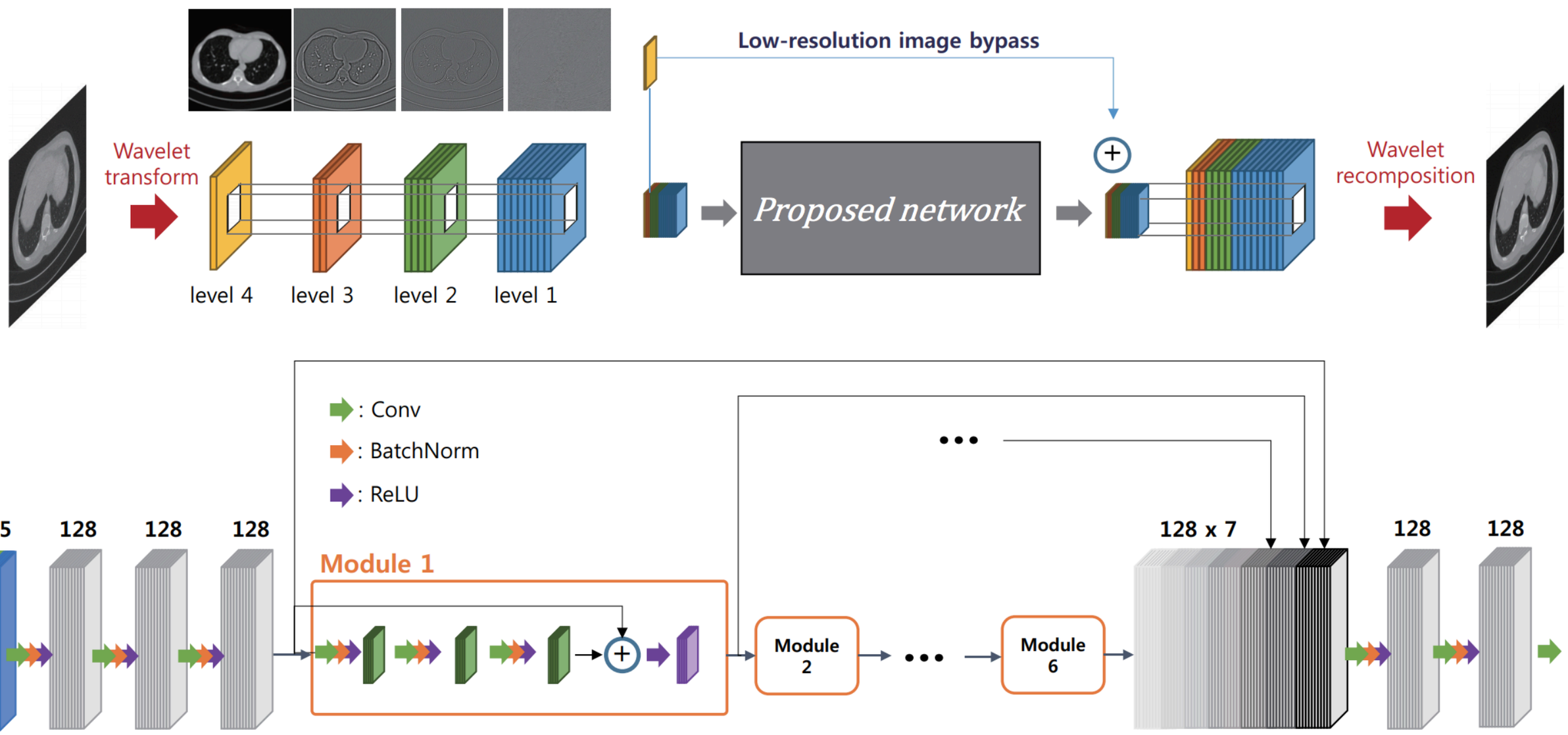

FIG. 5 Proposed deep convolutional neural network architecture for wavelet domain de-noising

Kang et al., A deep CNN for Low-dose CT reconstruction, Medical Physics, 2017

Fast MRI reconstruction

- Reconstruct high-resolution image from undersampled k-space data.
- Undersampled k-space = faster MRI acquisition.

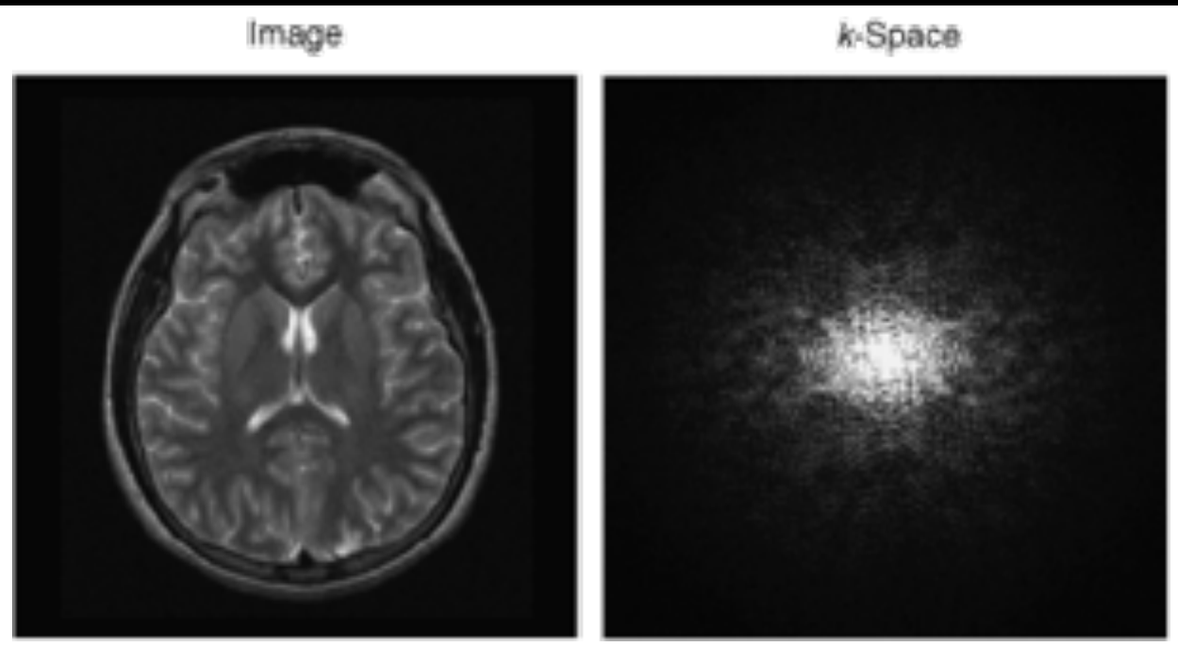

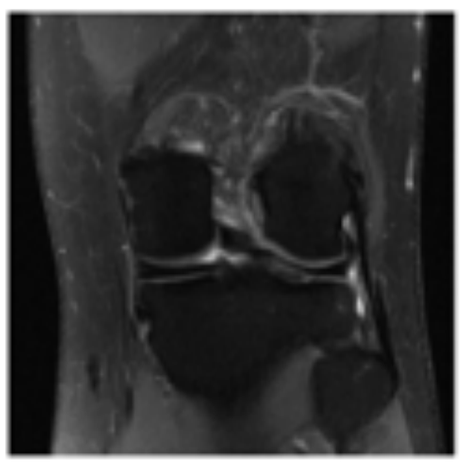

(a) Cropped and vertically flipped reconstruction from fully sampled k-space data

(b) Rectangular masked k-space

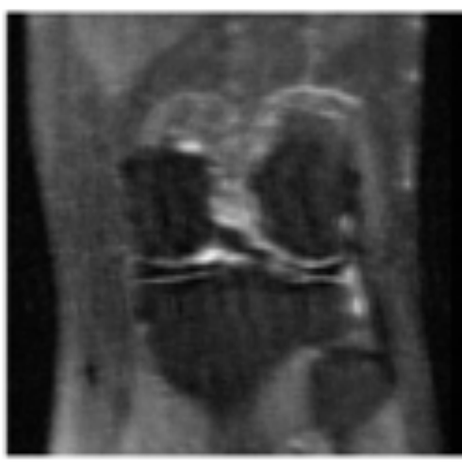

(c) Reconstruction via zero-filled IFFT

Image: fastMRI, Facebook + NYU, November 2018

Fast MRI reconstruction

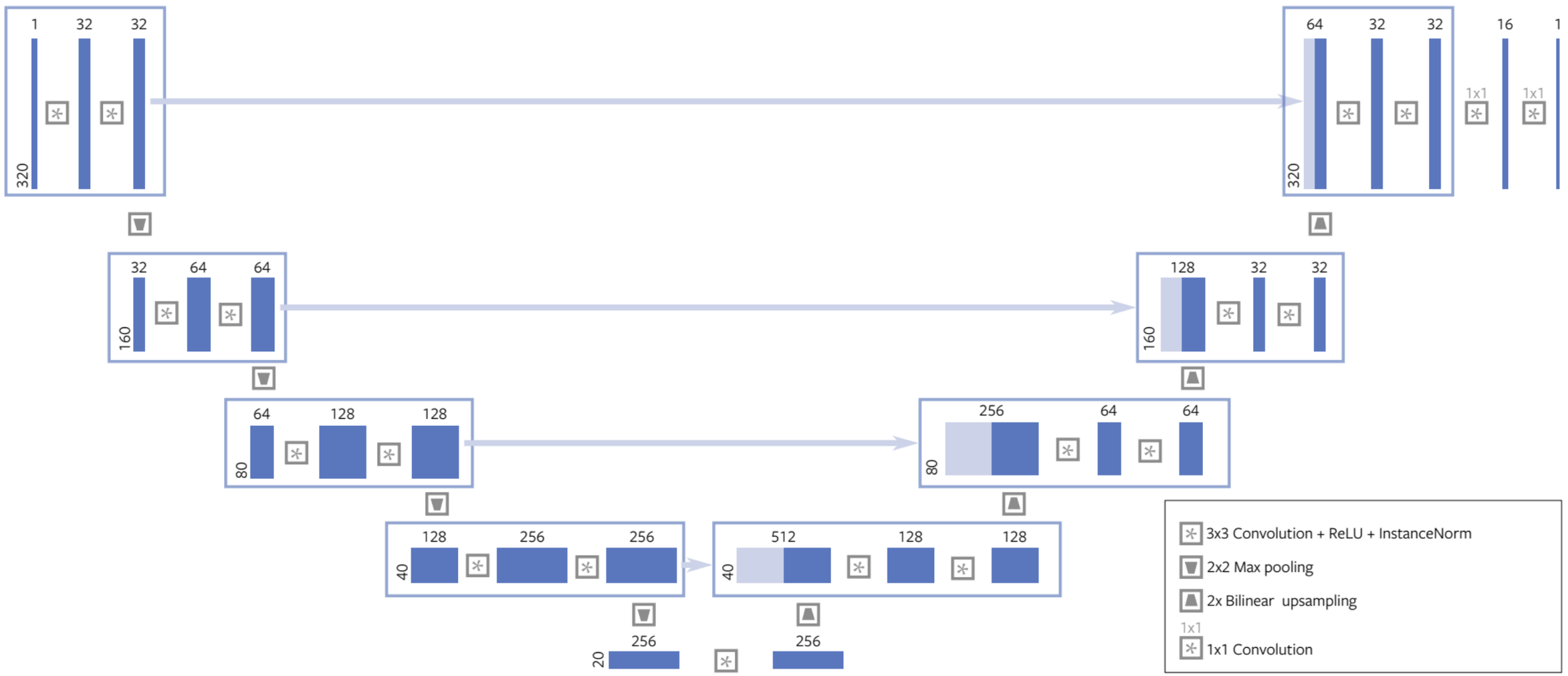

Figure 7: Single-coil baseline U-Net architecture

Image: fastMRI, Facebook + NYU, November 2018

Fast MRI reconstruction

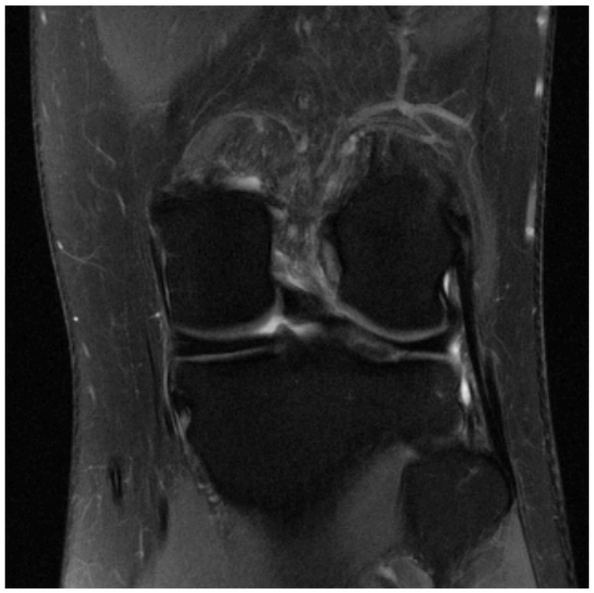

(a) Cropped and vertically flipped reconstruction from fully sampled k-space data

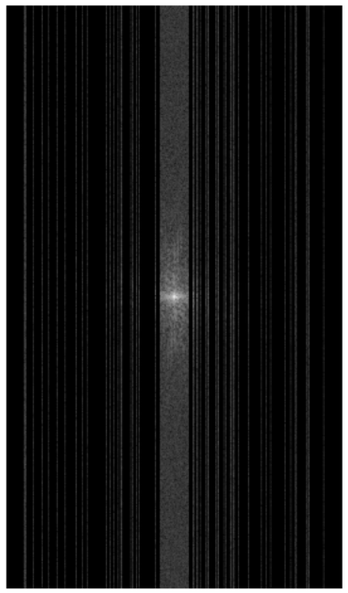

(b) Rectangular masked k-space

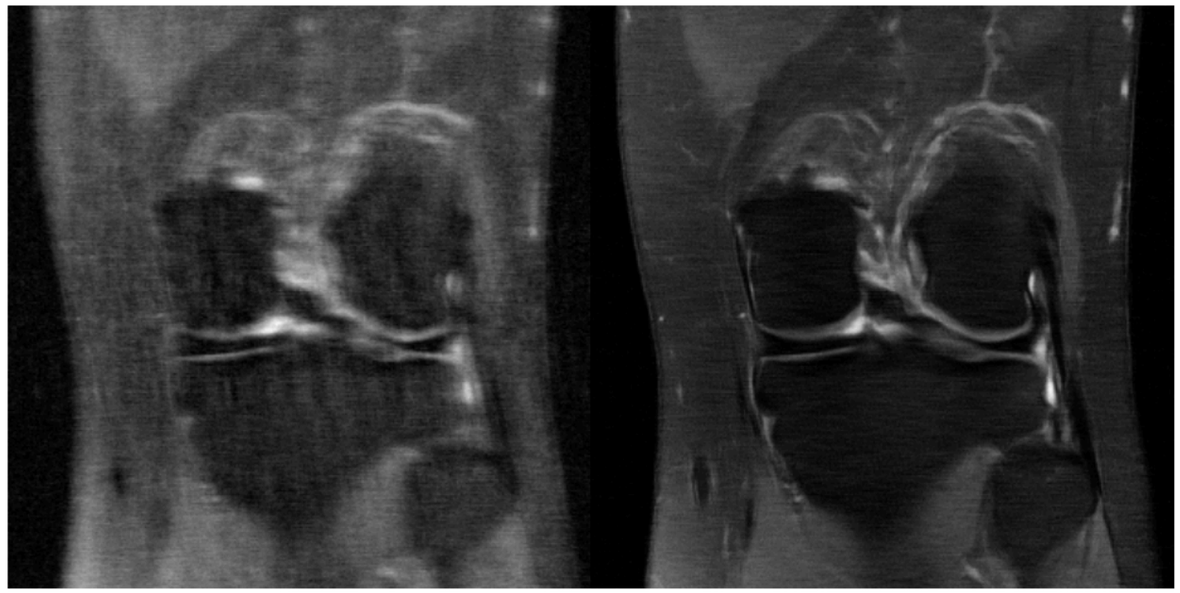

(c) Reconstruction via zero-filled IFFT

(d) Deep-learning baseline UNET reconstruction

Image: fastMRI, Facebook + NYU, November 2018

Poisson denoising

- The Poisson noise model is relevant in low-light scenarios.
- Using a model trained on the specific class of the image can boost performance.

Ground truth image | Noisy image | I+VST+BM3D [4] 24.45 dB | Proposed DenoiseNet 24.77 dB

Remez, Tal, et al. "Deep class-aware image denoising." 2017 international conference on sampling theory and applications (SampTA). IEEE, 2017

Poisson denoising

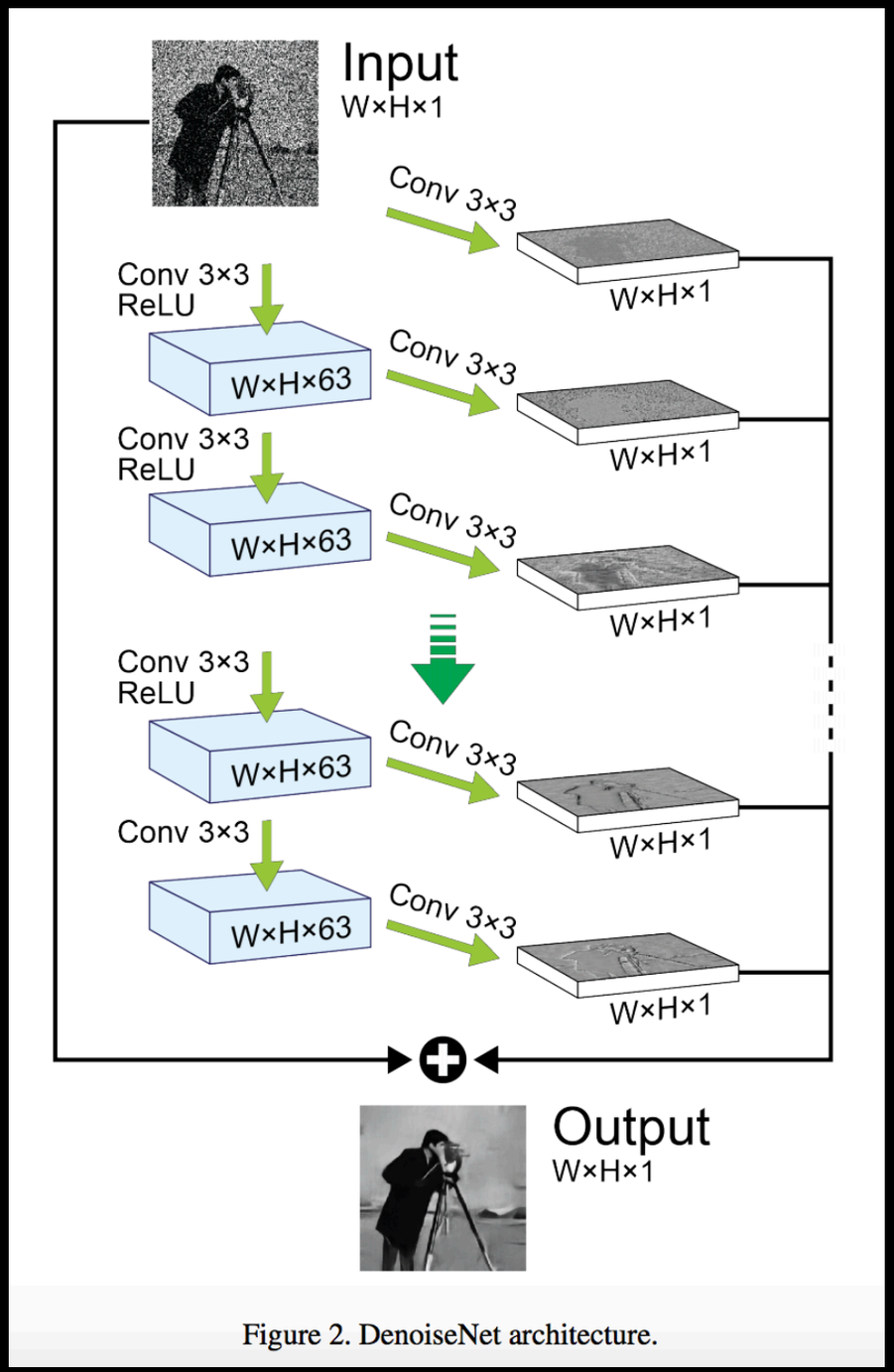

Figure 2. DenoiseNet architecture.

Remez, Tal, et al. "Deep class-aware image denoising." 2017 international conference on sampling theory and applications (SampTA). IEEE, 2017

Poisson denoising

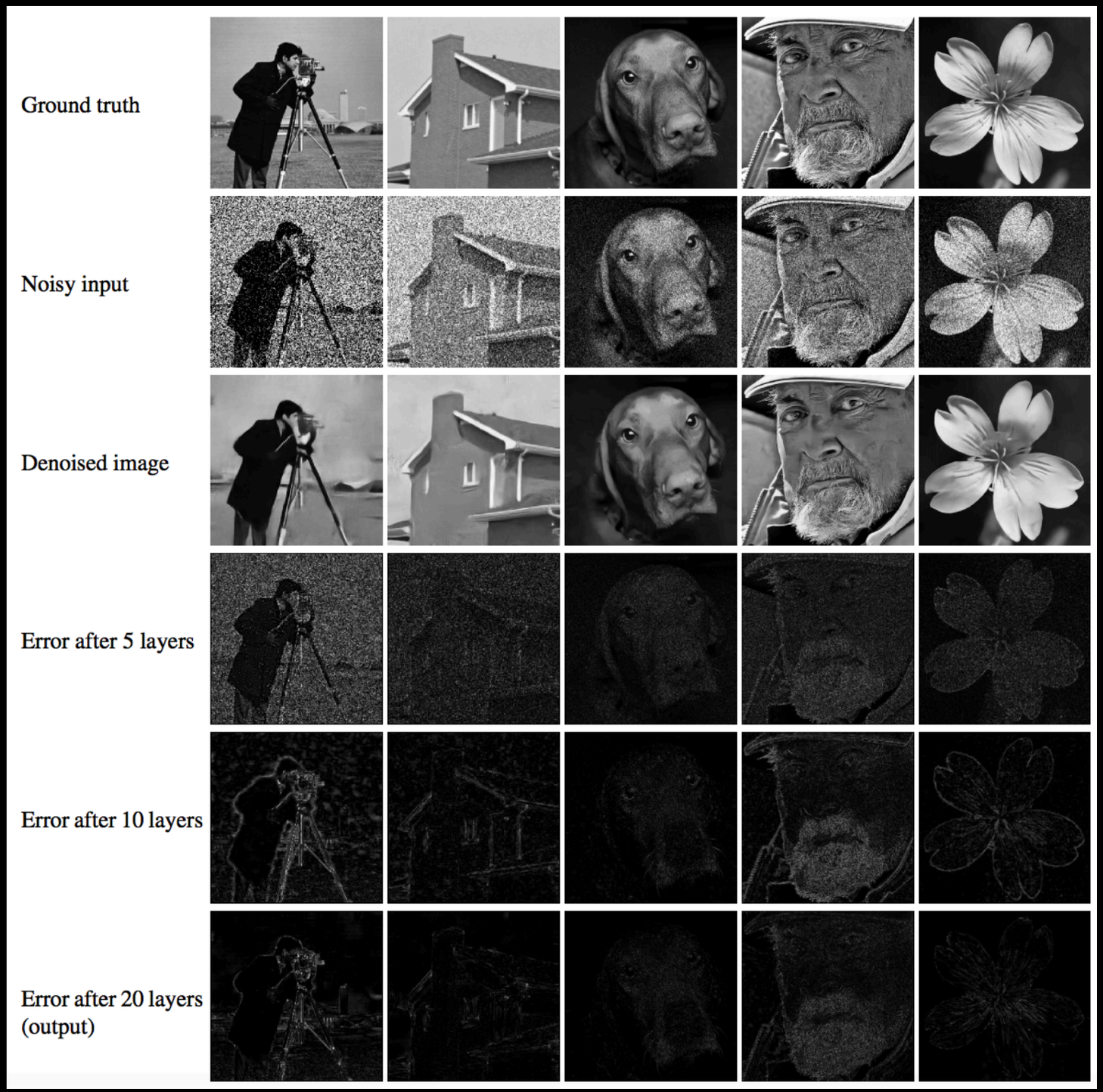

Remez, Tal, et al. "Deep class-aware image denoising." 2017 international conference on sampling theory and applications (SampTA). IEEE, 2017

DeepISP

- Learn a mapping from a raw low-light mosaiced image to a final visually compelling image.

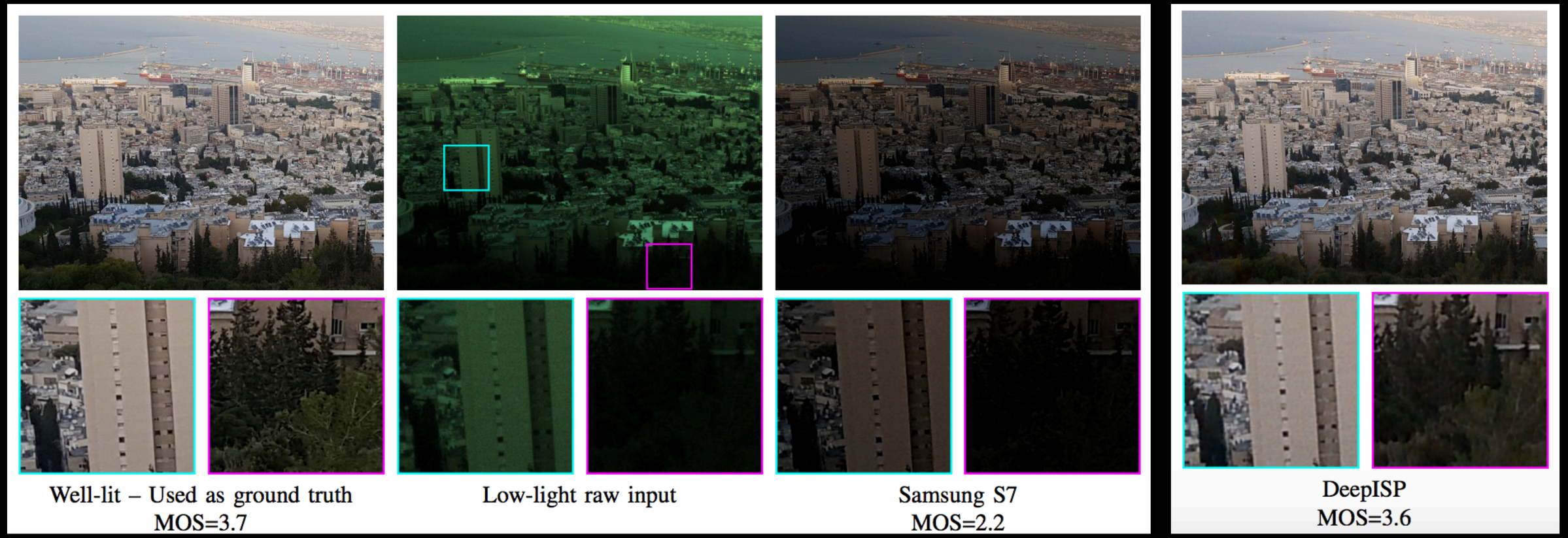

Schwartz et al., DeepISP, IEEE TIP, 2019

DeepISP

- Traditional ISP:
  - Low level: denoising, demosaicing.
  - High level: gamma correction, color correction.

- DeepISP:
  - Low level network
  - High level network

$$W \cdot triu\left(\begin{bmatrix} r & g & b & 1 \end{bmatrix}^T \cdot \begin{bmatrix} r & g & b & 1 \end{bmatrix}\right)$$

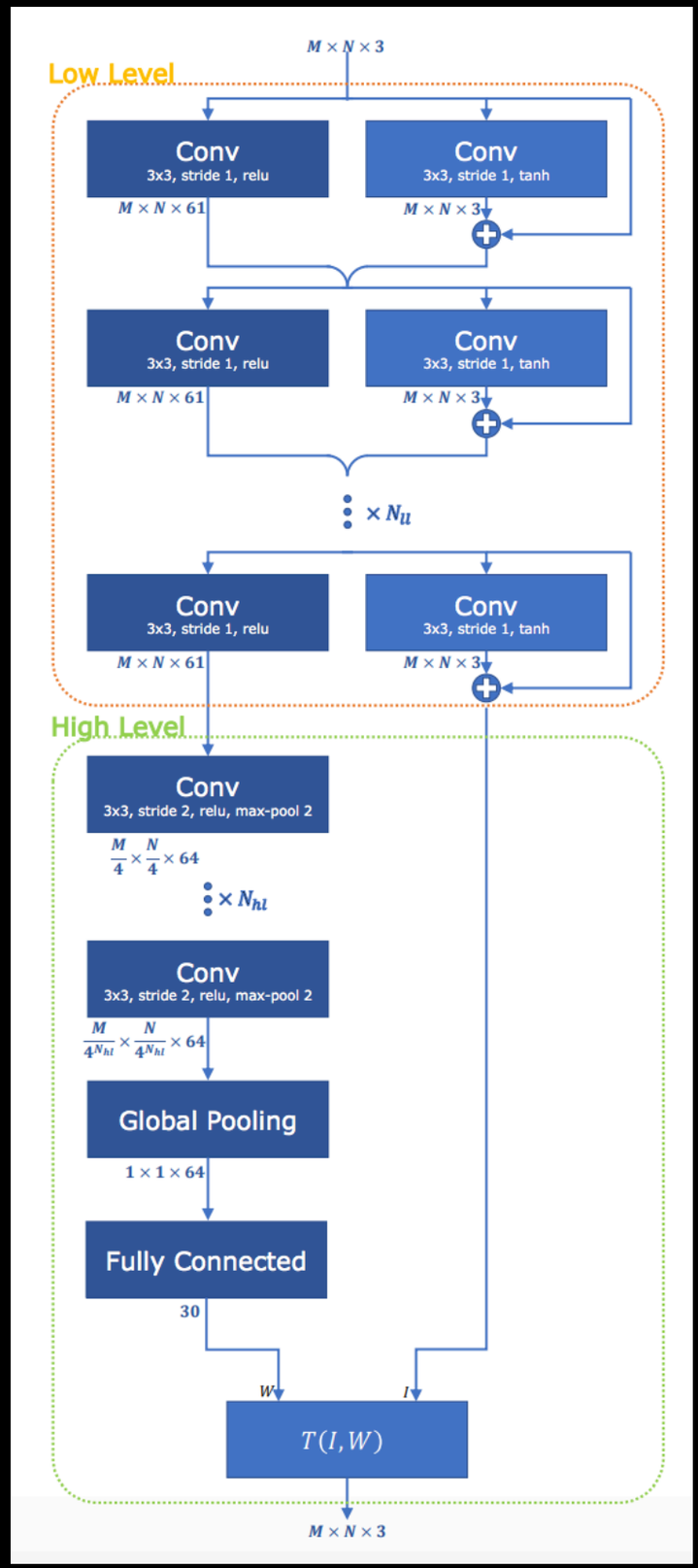

Schwartz et al., DeepISP, IEEE TIP, 2019

Deep burst deblurring

- Learn the weights for each Fourier coefficient in the burst.

$$u(\hat{\alpha}) = \mathcal{F}^{-1}\left(\sum_{i=1}^{N} w_i(\zeta)\hat{\alpha}_i(\zeta)\right)(x)$$

$$w_i(\zeta) = \frac{|\hat{\alpha}_i(\zeta)|^p}{\sum_{j=1}^{N}|\hat{\alpha}_j(\zeta)|^p},$$

$$u(\hat{\alpha}) = \mathcal{F}^{-1}\left(\sum_{i=1}^{N} h_\phi(\zeta)\hat{\alpha}(\zeta)\right)(x).$$

Wieschollek, Patrick, et al. "End-to-end learning for image burst deblurring." *Asian Conference on Computer Vision*. Springer, Cham, 2016

Deep burst deblurring

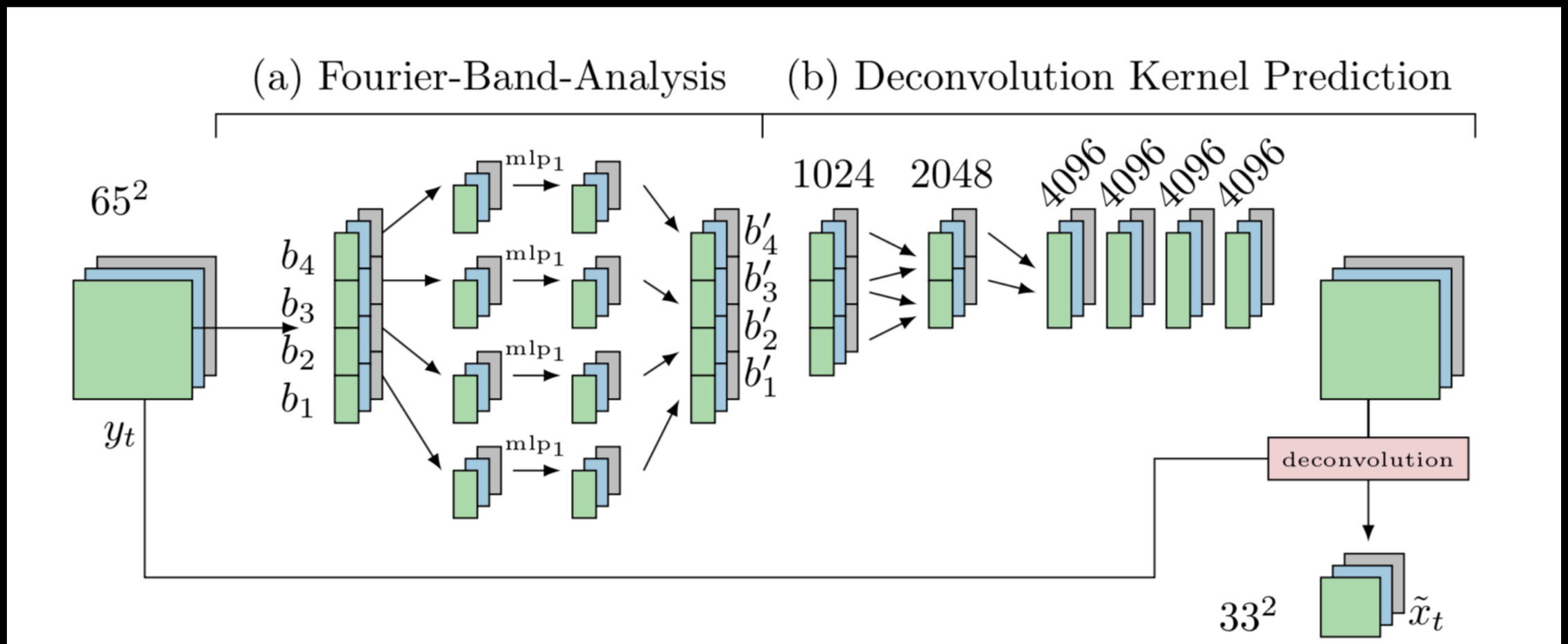

Fig. 1. Frequency band analysis and deconvolution for an image burst with 3 patches y_1, y_2, y_3. Following the work of Chakrabarti [11] we separate the Fourier spectrum in 4 different bands $b_1, \ldots, b_4$. In addition, we allow each band separately to interact across all images in one burst to support early information sharing. The predicted output of the deconvolution step are smaller patches $\tilde{x_1}, \tilde{x_2}, \tilde{x_3}$.

Wieschollek, Patrick, et al. "End-to-end learning for image burst deblurring." *Asian Conference on Computer Vision*. Springer, Cham, 2016

Deep burst deblurring

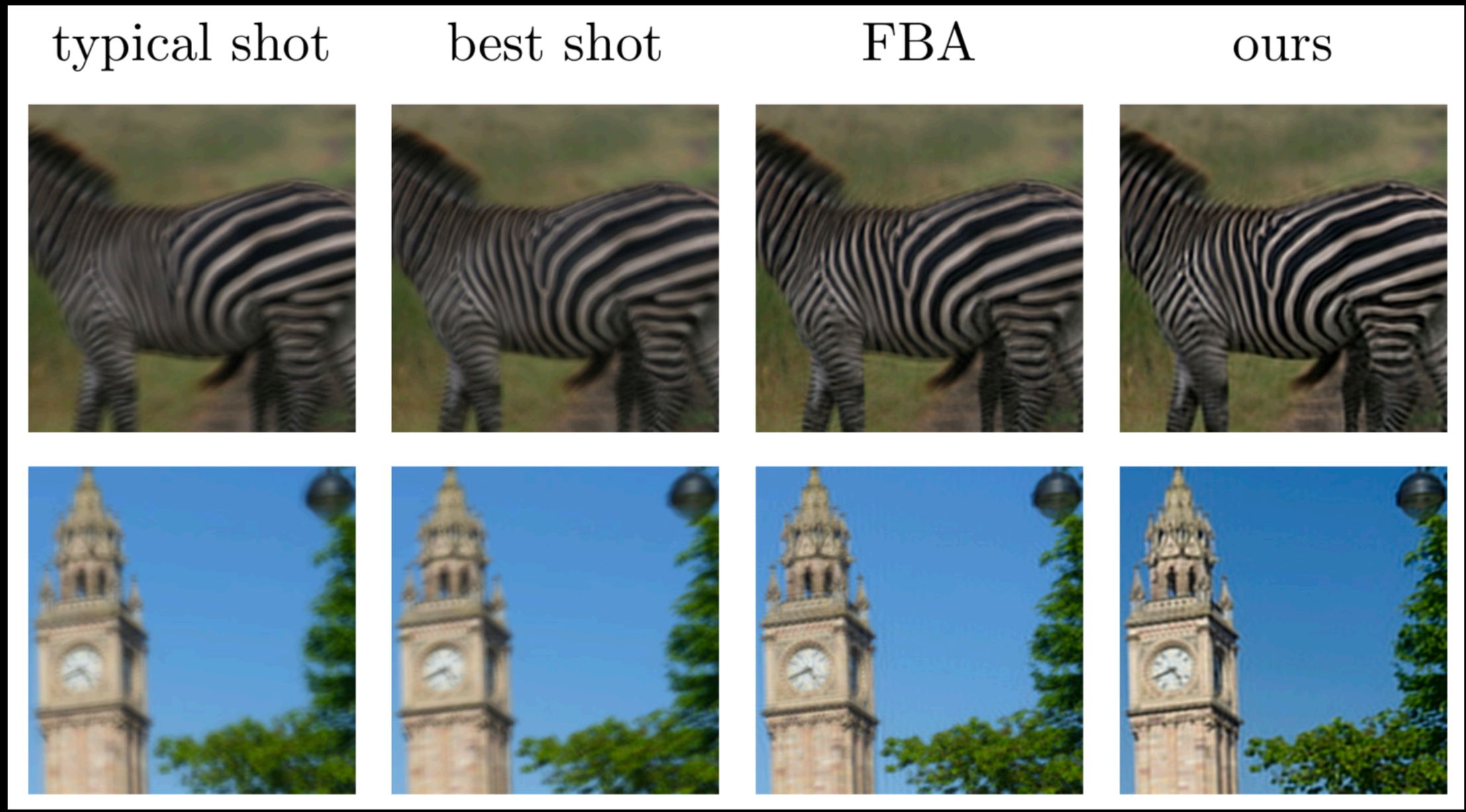

Wieschollek, Patrick, et al. "End-to-end learning for image burst deblurring." *Asian Conference on Computer Vision*. Springer, Cham, 2016